REPORT DOCUMENTATION PAGE

Form Approved
OMB No. 0704-0188

The public reporting burden for this collection of information is estimated to average 1 hour per response, including the time for reviewing instructions, searching existing data sources, gathering and maintaining the data needed, and completing and reviewing the collection of information. Send comments regarding this burden estimate or any other aspect of this collection of information, including suggestions for reducing the burden, to the Department of Defense, Executive Services and Communications Directorate (0704-0188). Respondents should be aware that notwithstanding any other provision of law, no person shall be subject to any penalty for failing to comply with a collection of information if it does not display a currently valid OMB control number.
PLEASE DO NOT RETURN YOUR FORM TO THE ABOVE ORGANIZATION.

1. REPORT DATE *(DD-MM-YYYY)*	2. REPORT TYPE	3. DATES COVERED *(From - To)*
7 July 2006	Final Technical Report	09/01/2002- 08/31/2005

4. TITLE AND SUBTITLE
Collaborative Center in Polymer Photonics

5a. CONTRACT NUMBER

5b. GRANT NUMBER
F49620-02-1-0428

5c. PROGRAM ELEMENT NUMBER

6. AUTHOR(S)
Professor Frank W. Harris (PI); (Co-I's) include Prof Stephen Cheng, Prof. Mark D. Foster, Prof. William J. Brittain; Prof. Thein Kyu; Prof. Sergei Lyuksyutov; Prof. Wayne Mattice; Prof. Alexei Sokolov, Prof. George Newkome; Prof. Roderic Quirk (for Liming Dai)

5d. PROJECT NUMBER

5e. TASK NUMBER

5f. WORK UNIT NUMBER

7. PERFORMING ORGANIZATION NAME(S) AND ADDRESS(ES)
The University of Akron
302 Buchtel Avenue
Akron, Ohio 44325-2102

8. PERFORMING ORGANIZATION REPORT NUMBER

9. SPONSORING/MONITORING AGENCY NAME(S) AND ADDRESS(ES)
AFOSR/NL
875 N. Randolph Street
Arlington, VA 22203

10. SPONSOR/MONITOR'S ACRONYM(S)

11. SPONSOR/MONITOR'S REPORT

12. DISTRIBUTION/AVAILABILITY STATEMENT
Approve for Public Release: Distribution Unlimited

AFRL-SR-AR-TR-06-0338

13. SUPPLEMENTARY NOTES

14. ABSTRACT
A Collaborative Center in Polymer Photonics (CCPP) that utilizes the collected research expertise of the AFRL Materials and Manufacturing Directorate and The University of Akron College of Polymer Science and Polymer Engineering in the development of polymers for photonic systems has been established. The Collaborative Center was formed so as to augment the Air Force Materials Laboratory in-house photonics research through team work with The University of Akron's polymer program (ranked second in the Nation by U.S. News and World Report). To this end, research teams made up of scientists from both institutions have been set up to pursue topics of mutual interest. This was made possible by funding by AFOSR ($900 k), AFRL ($900 k), and The University of Akron ($900 k). The Center has the capability to respond rapidly to new research directions as the needs of the Air Force change. It is also in a position to leverage resources from other sources such as the State of Ohio.

15. SUBJECT TERMS

16. SECURITY CLASSIFICATION OF:			17. LIMITATION OF ABSTRACT	18. NUMBER OF PAGES	19a. NAME OF RESPONSIBLE PERSON
a. REPORT	b. ABSTRACT	c. THIS PAGE			Frank W. Harris
				34	19b. TELEPHONE NUMBER *(Include area code)* 330-972-5459

Standard Form 298 (Rev. 8/98)
Prescribed by ANSI Std. Z39.18

Collaborative Center in Polymer Photonics

Introduction

A Collaborative Center in Polymer Photonics (CCPP) that utilizes the collected research expertise of the AFRL Materials and Manufacturing Directorate and The University of Akron College of Polymer Science and Polymer Engineering in the development of polymers for photonic systems has been established. The Collaborative Center was formed so as to augment the Air Force Materials Laboratory in-house photonics research through team work with The University of Akron's polymer program (ranked second in the Nation by U.S. News and World Report). To this end, research teams made up of scientists from both institutions have been set up to pursue topics of mutual interest. This was made possible by funding by AFOSR ($900 k), AFRL ($900 k), and The University of Akron ($900 k). The Center has the capability to respond rapidly to new research directions as the needs of the Air Force change. It is also in a position to leverage resources from other sources such as the State of Ohio. An important objective is the implementation of the Scientific and Technical Workforce for the 21st Century (STW-21) goals. To ensure that these objectives and goals are met, the following leadership team has been put in place: Gov't Program Manager: Lisa Denny; Gov't Technical Oversight: Dr. Barry Farmer; Gov't AFOSR Manager: Dr. Charles Lee; and UA Program Manager: Dr. Frank Harris.

The overall research goal of the Center is the development of polymer-based materials for photonic applications. This includes hybrid (organic/inorganic) and mixed (small molecule/polymers) systems. In this context, photonic applications are being pursued wherein the interactions between the material and electromagnetic radiation (light) is of paramount importance. The initial research focused on various aspects of the following topics: (1) 1-3 Dimensional Band Gap Systems (research team: Stephen Cheng & Frank Harris, UA Faculty; Tim Bunning, Rich Vaia & Barry Farmer, AFRL); (2) Nanotube Synthesis and Modification for Photonic Systems (research team: Liming Dai, UA Faculty; Rich Vaia, AFRL); (3) Surface Characterization in Photonic Systems (research team: Mark Foster & Alexei Sokolov, UA Faculty; Tim Bunning, AFRL); (4) Development of New Polymer Systems for Photovoltaic Devices (research team: Frank Harris, George Newkome, & Stephen Cheng, UA Faculty; Michael Durstock, AFRL); (5) Polymer Photonic Crystals Formed by Pattern-Photopolymerization (research team: Thein Kyu, UA Faculty; Tim Bunning, Rich Vaia, Seng Tan, AFRL/ML); (6) Simulations of Side-Chain Liquid Crystalline Polymers (research team: Wayne Mattice, UA Faculty; Barry Farmer, AFRL); (7) Development of Scanning Nano-Raman Spectroscopy for Characterization of Polymeric Nano-Structures (research team: Alexei Sokolov & Mark Foster, UA Faculty; John Maquire, AFRL); (8) Controlled Dispersion of Carbon Nanotubes in Polymeric Blends (research team: William Brittain & Liming Dai, UA Faculty; Rich Vaia, AFRL); and (9) Nanolithography in Polymeric Photonic Materials (research team: Sergei Lyuksyutov, UA Faculty; Rich Vaia, AFRL). Due to Professor Dai leaving The University of Akron, work on "Nanotube Synthesis and Modification for Photonic Systems" was discontinued and a new project on "Synthesis of Block Copolymers for Photonics Applications" (research group: Roderic Quirk, UA Faculty; Michael Durstock, AFRL) was initiated. The following is a summary of work carried out on the various research topics during the past three years.

Development of High Refractive Index Materials for the Fabrication of 3-D Photonic Crystals with a Complete Band Gap

Stephen Z.D. Cheng, Frank W. Harris, The University of Akron
Tim Bunning, Richard Vaia and Barry Farmer, AFRL

Photonic crystals (PCs) can quantum mechanically control the propagation and spontaneous emission of light, which can be used for ultra-fast switching, enhanced laser efficiency, and frequency filters among other potential applications, by means of a photonic band gap (PBG). Fabricating a photonic crystal requires a high refractive index material (n ~ 2.9) in a periodic arrangement where the periodicity is on the length-scale of the radiation one is trying to manipulate. Despite their advantages in terms of processing and fast non-linear optical responses, organics have not been used in 3D PCs because they do not have sufficiently high refractive indices. Poly(thiophene) (PT) is the only common polymeric system predicted to have a sufficiently high refractive index to open a complete 3D PBG because of its conjugation, and density.[1] PT is both insoluble and infusible, so to use this polymer in the fabrication of a PC, it needs to be synthesized as a thick film grown through a photonic template. The best way to make thick films of PT is by electropolymerization, but in practice this results in a film that has a substantially lower refractive index than predicted because of the "Poly(thiophene) Paradox".[2] This is where the oxidative potential needed to initiate the polymerization of the thiophene monomer (1.6V) is greater than the potential need to degrade the polymer (1.4V) resulting in low quality over oxidized PT films. It is known that one can stabilize the propagating cationic radical species with a polar aprotic lewis acid thereby reducing the initiation voltage of the thiophene monomer. Boron Triflurodiethyl Etherate (BFEE) was found to reduce the initiation potential to 1.3V enabling the synthesis of poly(thiophene) with a degree of polymerization (DP) of ~70, which is significantly higher than the DP of 14 previously achieved. This translated into a substantial improvement in the physical properties of the films including the tensile modulus (4 GPa) and the tensile strength (135 MPa). Despite the improvement in physical properties, the electronic properties of the poly(thiophene) did not significantly improve. FT-IR analysis (as seen in Figure 1a) showed that the thiophene monomer was being saturated and incorporated into the chain during the polymerization process. These saturated units both cut the conjugation length of the polymer, and introduce kinks into the chain which
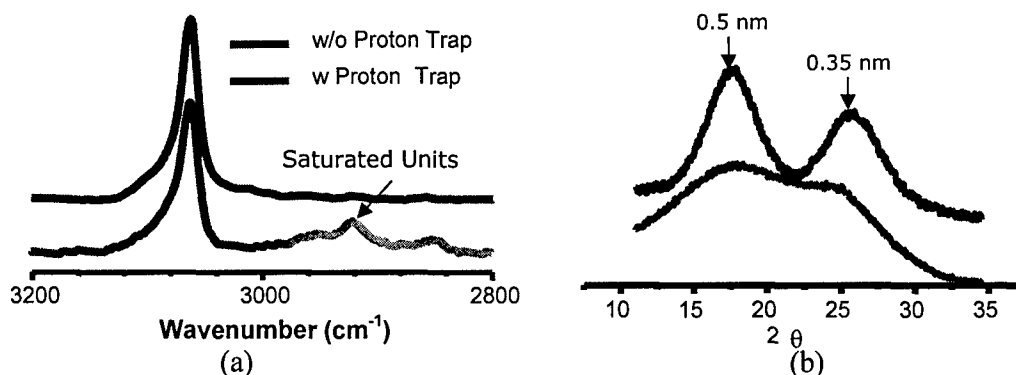

Figure 1: (a) FT-IR spectrum of PT showing reduced presence of saturated units with a proton trap. (b) XRD of PT indicating improved packing with a proton trap.

2

inhibited efficient packing. Together these reduced the optical and electrical properties of the film. It was determined that in addition to acidic protons being released during the polymerization, the BFEE solvent could react with water in the air creating even more acidic protons. These protons attacked and saturated the thiophene monomer. To prevent saturation, we introduced a proton trap into the reaction mixture to sequester the acidic protons. A series of proton traps were tested including 2,6 Di-*tert* butylpyridine; 2,4,6 Tri-*tert* butylpyridine, and 2,4,6 Tri-*tert* butylpyrimidine. All showed improvement in the electrical properties. FT-IR spectra of the PT films synthesized with a proton trap (see Figure 1a) showed a reduction in the number of saturated units. The concentrations of the components in the reaction mixture were then optimized with respect to the wavelength of maximum absorption of the PT film which correlates to the conjugation length of the chain. We were able to achieve a red-shift in the maximum absorption from 490nm to 501nm. This indicates a significant increase in the delocalization of the electrons. X-ray diffraction results (see Figure 1b) indicated a distinct increase in the sharpness of the diffraction peaks associated with the π-π stacking (0.35 nm) of the chains on top of each other and the lateral zipper packing (0.5 nm) of the chains. Improved packing increased the density of the PT from 1.49 g/cm^3 to 1.51 g/cm^3 It is also known that lower temperatures promote α-α linkages over α-β linkages of the thiophene which permits increased conjugation and greater regularity in the polymer chain. In light of this, we re-optimized the reaction mixture for polymerization at −50°C which is 8°C above the freezing point of the solvent. This resulted in a red-shift of the maximum absorption wavelength to 521 nm. We then used variable angle ellipsometry to determine the optical constant in the absorbing

Figure 2: Optical constant dispersion curve for PT

region and an interference fringe method to obtain refractive index values at longer wavelengths. All of the improvements translated into significantly improved refractive indices. It was determined that we could achieve a maximum refractive index value of ~3.36 and an off-resonance value of about 2.5-2.6. This is the first time that an organic system has been report to have a refractive index sufficiently high to open a complete 3-D PBG with a standard hard sphere inverse fcc structure. In fact, using an optimized fcc structure which has a refractive index contrast threshold of ~2.5, PT can open up a complete 3-D PBG across a large range of wavelengths.[3] This development opens up the possibility of being about to exploit the benefits of organics in 3D PCs.

The next step was to create a photonically active template to grow the high refractive index PT through. The most common method used is the colloidal crystallization of spheres with diameters on the length-scale of the light where the PBG will be. In particular, we used Colvin's method to create fcc colloidal films with thicknesses of greater than 9 unit cells required to open a PBG.[4] Because Colvin's method is inherently kinetic, defects get incorporated into the structure. At sufficient

concentrations and appropriate distributions defects can close a PBG. To reduce the effect of defects on the PCs optical response, we have developed a technique to reduce the defect levels and increase perfection in entropy-driven structures called nano-mechanical annealing. In this process, the colloidal crystal is placed on a piezo-electric element and a voltage wave is sent across the element causing vibration. By controlling the frequency and amplitude of the wave, the crystal can be shook at a specified rate and height. Using this we have observed that the spheres improved their packing regularity and defects independent of any attractive or repulsive forces aggregated together effectively decreasing their concentrations. Currently, no theory concerning colloidal crystals addresses why this should occur. To better understand why unassociated interactionless defects would aggregate, we developed a model of the surface dynamics of the spheres on a surface with hexagonally arranged potential wells to describe the motion of the spheres on the top layer of the colloidal crystal. The model confirmed that the defect aggregates should form and the defect levels predicted by the model correspond within a few percent to the observed
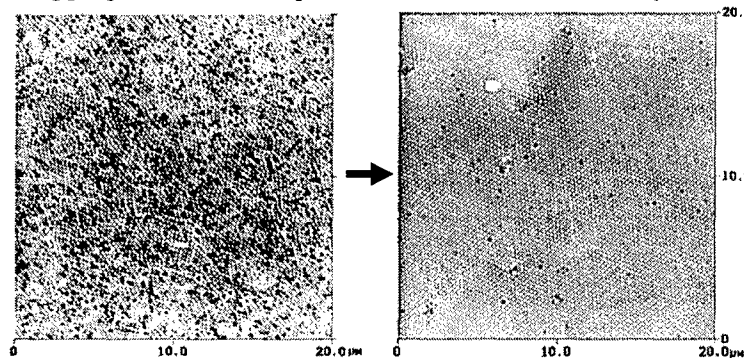

Figure 3: AFM pictures of a colloidal crystal before and after mechanical annealing

defect concentrations with only one fit parameter. This aggregation was found to be driven by the spheres trying to maximize high energy modes of motion on the surface. This is an important finding in that it shows that in entropy driven systems with geometrically isotropic units in a uniform potential field, defects will spontaneously aggregate. This concept can be used in understanding the development of other self-assembling systems.

Over the course of this project we have made to major contributions of interest to the Airforce in the field of photonics. First, we developed a synthesis route for a PT system which exhibited refractive index values unprecedented in organic materials and sufficiently high to open up a complete 3D photonic band gap. This starts to open the area of higher dimensional PCs to the physical properties and performance advantages of organics. The second contribution was to the understanding of entropy driven structure perfection. We developed a nano-mechanical annealing technique to perfect colloidal crystal structures and have modeled the surface dynamics to understand the mechanism of this perfection process. These are the two critical foundations for the next step of the project; combining the high refractive index PT with the colloidal crystal template to achieve for the first time an all organic 3D photonic crystal with a complete PBG.

1. Yang, C.; Jenekhe, S. *Chem Mater.* **1995**, *7*, 1275.
2. Hamnett, A.; Hillman, A. R. *J. Electrochem. Soc.* **1988**, *135*, 2517.
3. Busch, K.; Johns, S. *Phys. Rev. E* **1998**, *58*, 3896.
4. Jiang, P. et al *Chem. Mater.* **1999**, *11*, 2132.

4

Characterization of Photonic Film Structure and Its Dependence on PECVD Process Parameters
Period 9/1/02 – 8/31/05
M.D. Foster, S. Peri, The University of Akron

We have collaborated with Tim Bunning and Hao Jiang at the Air Force Research Laboratory to perform ground-breaking experiments using reflectometry and off-specular scattering with films created using plasma-enhanced chemical deposition. These studies have uncovered a wealth of information about the structure of these novel and useful films.

Single Layer Films: Our study began with the elucidation of the structure of single films and multilayer structures in which each layer was created at plasma power of 30W using a single precursor, either octafluorocyclobutane (OFCB) or benzene (B)1. Layers of sharply different refractive index can be made with these two precursors, allowing passive optical filters to be constructed from multilayers. The first key finding was that the structure of a plasma-polymerized OFCB film (PP-OFCB) immediately adjacent to an oxide-covered silicon substrate is different from that in the remainder of the film due to a transient in deposition behavior. Using neutron reflectometry together with X-ray reflectometry as complementary techniques was critical to uncovering this feature. When the material begins to deposit, it "sees" an oxide surface and the polymer formed is deficient in fluorine as compared to the remainder of the film. Once the oxide is covered a different structure is deposited and the resulting transition in film structure occurs over a very small depth, about 0.6 nm. This transient is deposition behavior is not universal, but dependent on the details of the plasma polymerization chemistry, as it is not seen in the deposition of films from benzene precursor.

Under these processing conditions, homopolymer films of benzene are extraordinarily smooth for thicknesses up to 400 nm. They are considerably smoother that polymer melt films of the same thickness. The roughness of these benzene homopolymer films is essentially unchanging over thicknesses up to 400 nm. This lack of change is also remarkable and stands in contrast to the so-called kinetic roughening seen with other sorts of processes for depositing films. OFCB homopolymer films are also very smooth for thicknesses up to 400 nm., but the roughness does change with thickness, though very slowly, more slowly than reported for any other type of solid film having surface roughness dictated by deposition method. Additional information about the roughness of these films can be obtained by performing X-ray off-specular scattering measurements which are sensitive to lateral variations in structure. The form of the off-specular scattering from the benzene films tells us that what roughness is present occurs mostly on length scales smaller than about 60 nm, but the character of the roughness is somewhat variable with thickness. On occasion we see grazing incidence small-angle scattering from the benzene homopolymer films. This points to some sort of micron scale structure on or within the film. The form of the off-specular scattering from the OFCB homopolymer films tells us that what roughness is present occurs mostly on length scales smaller than about 60 nm.

Multilayer Films: In bilayer films and multilayer films with alternating layers of plasma-polymerized benzene (PP-B) and plasma-polymerized OFCB (PP-OFCB), the

details of the interface profile between each pair of layers were resolved using X-ray and neutron reflectometry. All the interfaces are sharp and well-defined by optical standards and off-specular scattering measurements indicate that the structures of the interfaces are strongly correlated to one another over the length scales to which the X-ray measurements are sensitive. The average interface width, a_I, between layers made from the different precursors is about 4 nm (1.6 nm rms). The layer/layer interfaces are generally 2-3 times broader that the layer/air interfaces.

Copolymer Films: Additional advances in the manufacture of photonic layers with arbitrary refractive index profiles can be made if one can deposit "copolymer" films made using mixtures of two precursors. The first detailed structural studies of such copolymer films have also been carried out in this work. In copolymer films of benzene and OFCB a transition region is seen adjacent to the substrate if the OFCB content is large enough. The importance of this transition region diminishes as the OFCB content diminishes. Copolymer films of OFCB and hexamethyldisiloxane (HMDS) have also been studied, and to support that work HMDS homopolymer films were studied as well. A transition region adjacent to the substrate is also seen for HMDS homopolymer films and for OFCB-HMDS copolymer films, though the behavior in the copolymer films is more complex.

Atomic Force Microscope (AFM) imaging of the film surfaces complements the scattering investigations, since microscopy provides a highly local, direct image of the surface, while scattering techniques provide a statistical picture of structure averaged over mm^2 or cm^2. In figure 1 are the 565 nm x 565 nm topographic, phase, and amplitude images for an HMDS homopolymer film measured in intermittent contact mode. A key feature of the generally very smooth surface is the presences of nanoparticles on the surface. As the fraction of comonomer OFCB is increased, the particles on the surface become much smaller and then disappear, suggesting that copolymerization disrupts the means by which these particles are formed
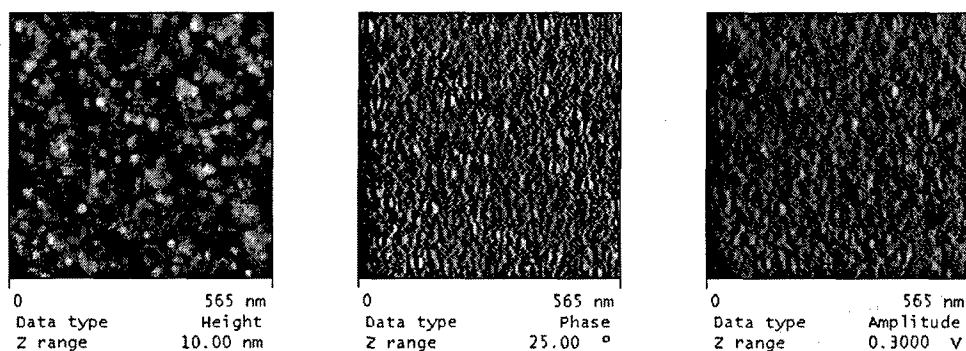

0	565 nm	0	565 nm	0	565 nm
Data type	Height	Data type	Phase	Data type	Amplitude
Z range	10.00 nm	Z range	25.00 °	Z range	0.3000 V

Figure 1: Image of PP-HMDS homopolymer at a scan size of 565 nm.

Variations with Processing Parameters: After uncovering these details of structure for films made at comparatively low plasma power, we initiated a systematic study of the variation in the film structure with variations in processing parameters. Benzene homopolymer films made at higher plasma powers show a surface layer of 7-10 nm thickness that is enriched in oxygen. The existence of the surface layer exists was shown independently with reflectometry and XPS.

Both the overall level of crosslinking and the variation in crosslink density with depth can be sensitively probed by swelling the film with solvent vapor and determining the change in layer thickness and distribution of solvent in the film with reflectometry. Experiments run on PP-OFCB films and PP-B films make it clear that crosslink density can vary sharply between films made at the same reactor conditions with different precursors. However, even for a given precursor the crosslink density varies markedly with deposition conditions such as plasma power. In figure 2 is plotted a profile of neutron scattering length density (SLD), $(b/V)_n$, with depth for a PP-OFCB film swollen in deuterated tetrahydrofuran. Near a depth of zero, corresponding to the interface with the substrate, the SLD is high, indicating enrichment in solvent. The solvent concentration drops as one moves toward the air interface, indicating a higher crosslink density near the surface.
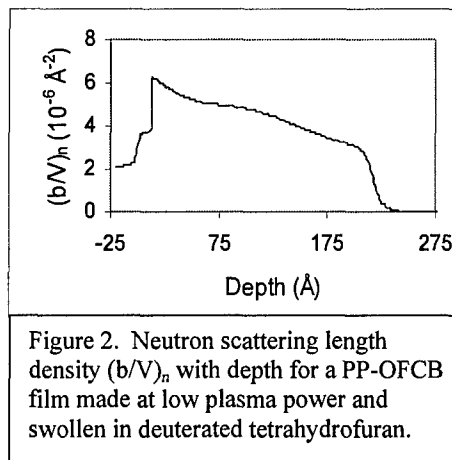
Figure 2. Neutron scattering length density $(b/V)_n$ with depth for a PP-OFCB film made at low plasma power and swollen in deuterated tetrahydrofuran.

When the various types of homopolymer films are swollen with solvent, good attachment of the film to the substrate is maintained. However, attachment to the substrate is not good for some copolymer films, indicating that the copolymerization changes the covalent reaction of the growing polymer with the silicon oxide. First measurements of the kinetics of the film swelling have been made.

Emerging Techniques: While the research has brought a better understanding of the structure of PECVD films pertinent to building photonic films, it has also provided the opportunity for introducing emerging techniques to the study of materials of interest to the Air Force. In the third year, grazing incidence small angle x-ray scattering, GISAXS, was applied to photonic multilayers for the first time. GISAXS measurements reveal very rapidly qualitative information about the degree of correlation between interfaces in a multilayer film and can be analyzed to yield detailed information on the correlation. The use of GISAXS in characterization of photonic films will make possible much more sophisticated global characterization of the interface structure, with the key challenge being to develop facile methods and software for the analysis of the large data sets.

Student Training: A third aspect of the research has been the exposure of students to research in photonics and the Air Force's interests. This student involvement was expanded beyond graduate students in the third year by including a strong undergraduate summer researcher, Brian Habersberger, whose stipend was supported by UA's NSF-funded Research Experiences for Undergraduates program.

Future work: We propose that future research should focus on further defining the variation in film structure, particularly crosslinking, with plasma power, monomer feed location, monomer type, and substrate type. Studying the development of surface roughness with increasing thickness at different polymerization conditions will aid efforts to identify optimal processing conditions for creating photonic multilayers meeting Air Force needs. The kinetics of swelling will also be investigated to more precisely describe the interaction of these films with solvents and the character of the crosslinking.

Discotic Liquid-Crystalline Heterocyclics for Photovoltaic Applications

Frank W. Harris and Stephen Z.D. Cheng

The object of this research was the design, synthesis and evaluation of fused-ring, discotic liquid-crystalline heterocyclics for use as electron transporting materials in photonic devices. The work was begun with the synthesis of a series of organo-soluble, 2,6,7,11,15,16-substituted bisphenazines. The bisphenazines were obtained in 70-80% yields from the condensation of 2,7-disubstitutedpyrene-4,5,9,10-tetraones and 1,2-diamino-4,5-dialkoxybenzenes. The molecules have eight fused aromatic rings including two phenazine rings with two alkyl groups located at the 2- and 11- positions and four alkoxy groups located at the 6-, 7-, 15-, and 16- positions. Differential scanning calorimetry (DSC), polarized light microscopy (PLM) and wide-angle X-ray diffraction (WAXD) studies showed that some of these planar molecules display liquid-crystalline phases at temperatures ranging from over 300 °C to 120 °C. The liquid-crystalline temperature range was manipulated through variation of the alkyl chain substituents at either the 6-, 7-, 15-, 16- or 2-, 7- positions. WAXD analysis also indicated that the molecules undergo π-π stacking in the liquid-crystalline phase. The π-π stacking distance was calculated to be 3.6 Å. Cyclic voltammetry (CV) showed that the compounds undergo two reduction processes at -2.04 V and -2.14 V (vs. Fc/Fc$^+$). The electron affinity of the compounds was 2.76 eV. The alkyl chain substituents had no significant effect on either the electro-optical or electro-chemical properties. A photovoltaic cell from a blend of poly(3-hexylthiophene) (P3HT) and one of the bisphenazines showed an open-circuit voltage of 0.90 V, which was about 45 times higher than that of a cell made from pure P3HT.
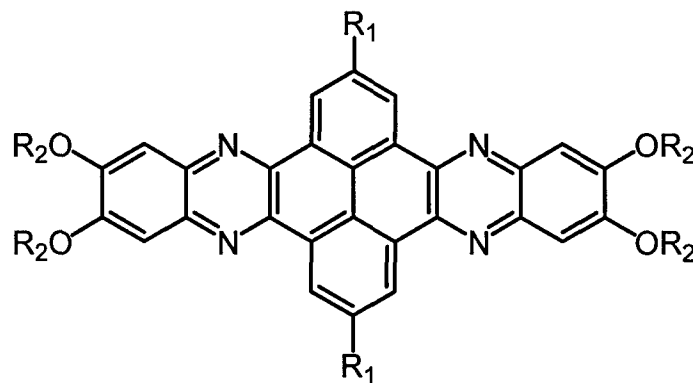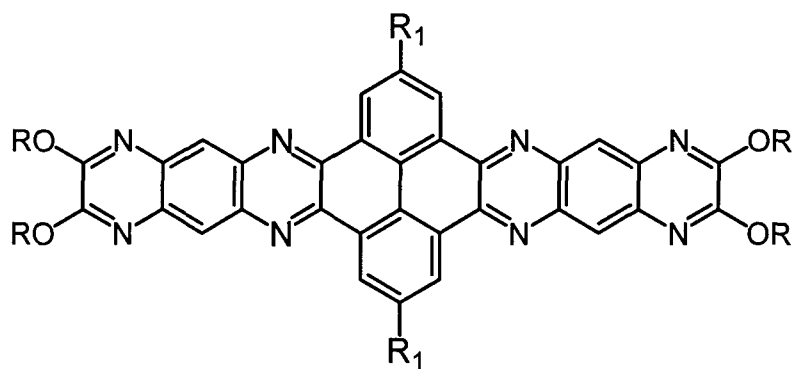

Series 1

To avoid the multi-step preparation of pyrene-4,5,9,10-tetraone and 2,7-disubstituted-pyrene-4,5,9,10-tetraones, the oxidation of pyrene and the 2,7-dialkylpyrenes was reinvestigated. The pyrenetetraones were successfully prepared in one step through ruthenium(III)chloride catalyzed oxidation using sodium periodate as

the oxidant. Interestingly, the oxidation could also be controlled to selectively afford pyrene-4,5-diones using less amounts of oxidant and lower reaction temperatures.

Functionalization of pyrene at the 2- and 7- positions was carried out via electrophilic substitution of 4,5,9,10-tetrahydropyrene, which is the reduction product of pyrene. Previous routes to 4,5,9,10-tetrahydropyrene always led to a mixture of the desired compound and other impurities, which are extremely difficult to separate. This work reinvestigated the reduction of pyrene. Birch reduction of pyrene gave 4,5-dihydropyrene, which was reduced further to 4,5,9,10-tetrahydropyrene using in-situ formed sodium ethoxide in toluene. The purity of the final compound was over 90%, which is the best ever reported. The overall yield of these two reactions was over 80%.

In an attempt to obtain materials with lower reduction potentials, a second series of heterocyclics (tetraphenazines) with increased conjugation length and containing more nitrogen atoms was designed and prepared. The compounds were obtained by treating 2,7-di-t-butylpyrene-4,5,9,10-tetraone with 2,3-dialkoxy-6,7-diaminoquinoxalines. The tetraphenazines have ten fused aromatic rings including four fused phenazine rings with two t-butyl groups located in the 2- and 13- positions and four alkoxy groups located in the 7-, 8-, 18- and 19- positions. The compounds, which underwent reduction at -1.74 V and at -1.90 V (vs. Fc/Fc$^+$), displayed liquid-crystalline phases from 160 to over 250 °C. The molecules also underwent π-π stacking in the liquid-crystalline phase. The π-π stacking distance was calculated to be 3.6 Å. The electron affinity of the compounds was 3.06 eV.

Series 2

A third series of disc-shaped compounds (the hexaphenazines) were prepared by condensation of hexaketocylcohexane with 2,3-dialkoxy-6,7-diaminoquinoxalines. This group of molecules contained six fused phenazine rings. The hexaphenazines had six alkoxy groups located at the 4-, 5-, 12-, 13-, 20- and 21- positions. The molecules displayed two crystalline phases, but no liquid-crystalline phases. The phase behavior was strongly dependent on the cooling or heating rates. Interestingly, these molecules

9

underwent three reduction processes at -1.38 V, -1.47 V, and -2.20 V (vs Fc/Fc$^+$). The electron affinity of these molecules was 3.42 eV. This indicates that they are relatively strong electron-acceptors.
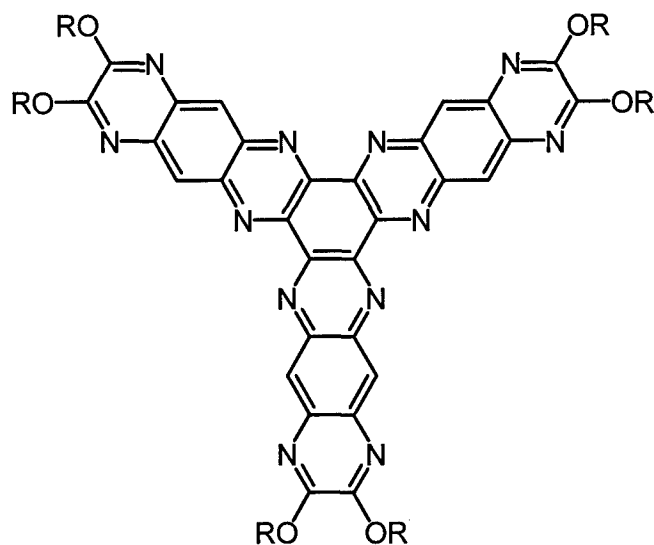
Series 3

Summary of Research Accomplishments in T. Kyu group:

The research emphasis of the PI group (T. Kyu) was directed to elucidation on formation of holographic polymer dispersed crystals and photonic crystals both experimentally and theoretically in collaboration with Tim Bunning's group at the Wright Patterson Air Force. The PI group published 5 papers and delivered 8 presentations plus 3 invited talks at the national and international meetings.

Holographic Polymer Dispersed Liquid Crystals

The modeling part was done initially for a single component system using the classical reaction-diffusion equation pertaining to the concentration of emerging polymer. It was found that molecular transport seems to control the pattern forming aspect of H-PDLC. The accomplishment was documented in a paper entitled "Transport Controlled Pattern Photopolymerization in a Single-Component System." S. Meng, K. Nanjundiah, T. Kyu, L. V. Natarajan, V. P. Tondiglia, and T. J. Bunning, Macromolecules, 37, 3792-3798 (2004). The theoretical model has been modified for a binary blend containing photo-reactive monomer and liquid crystals. The modification was necessary because the classical reaction diffusion equation has been erroneously applied to the phase separating binary system. We have shown that the Cahn-Hilliard dynamics having a double well potential must be used to describe the pattern formation in binary blends as opposed to the single-well potential that has led to the reaction diffusion equation utilized a single component system.

Modeling and Simulation of tunable photonic crystals in mixtures of photo-curable monomers and liquid crystals via pattern photo-polymerization has been completed in two dimensions. The linkage was made between structural development and diffraction efficiency of the resultant photonic crystal. The simulated results conform well to the experimental findings, which justifies the accountability of the theoretical predictions. Based on the structure-property relationship established by the PI's group, one is able to estimate the optimal fabrication conditions such as laser intensity, mixture composition, radiation time, before doing any experiments. It may substantially reduce the amount of time, resource, and manpower in the programs with AFOSR to develop advanced materials with electro-optical applications. This part of the project has been carried out in collaboration with Sutherland and Bunning's group at WPAFB. This collaboration resulted in a joint paper entitled: The present work is the first to demonstrate the diffraction efficiency (DE) of gratings, a key property in electro-optical applications, which can be predicted directly from the simulated morphology evolution of the holographic polymer-dispersed liquid crystals (H-PDLC) via our coarse-grain modeling. The accomplishment has been summarized in a paper entitled "Holographic photo-polymerization induced phase separation in reference to the phase diagram of a mixture of photo-curable monomer and nematic liquid crystal." S. Meng, T. Kyu, L.V. Natarajan, V. P. Tondiglia, R.L. Sutherland, and T.J. Bunning, Macromolecules, 38, 4844-4854 (2005). A review paper has been published in a refereed Korean journal entitled "Holographic Polymer Dispersed Liquid Crystals and Polymeric Photonic Crystals formed by Holographic Photolithography," T. Kyu, S. Meng, H. Duran, K. Najundiah, and G.R. Yandek, Macromol. Res., 14, 155-165 (2006).

Currently, PI's group is examining the effect of reaction kinetics of photo-polymerization on diffraction efficiency properties during fabrication of tunable photonic crystals via lithography. P-DSC and FTIR experiments have been conduct to obtain the experimental parameters for simulation. This study is well in line with other programs with AFOSR (i.e. Guymon's project on

photo-polymerization reaction kinetics in mixtures of liquid crystal/photosensitive monomers). It will render fundamental understanding and better appreciations of the experimental findings from that project. This part of the project has been carried out in collaboration with Sutherland, Tondiglia, Natarajan, and Bunning at WPAFB.

Polymer Photonic crystals

We have extended the H-PDLC study to the simulation has been successfully extended to the fabrication of three-dimensional photonic crystals via holographic lithograph. It is capable of guiding the experimentalists to use the appropriate optical set-up for the desired photonic structures (i.e. BCC, FCC). In addition, PI's group investigated the effect of network elasticity. The theoretical findings suggest that the flexible HEMA, thiolenes structures are preferred over the rigid acrylic monomers, giving chemists some hints as to what chemical structures to synthesize for preferred properties of tunable photonic crystals. This finding is consistent with the findings by J. Natarajam et al in the thiolene based H-PDLC system. A paper has been published: "Formation of Electrically Switchable Photonic Crystals via Various Optical Wave Interference Techniques" G.R. Yandek, S. Meng, G.M. Sigalov, and T. Kyu, Liq. Cryst., in press (2006).

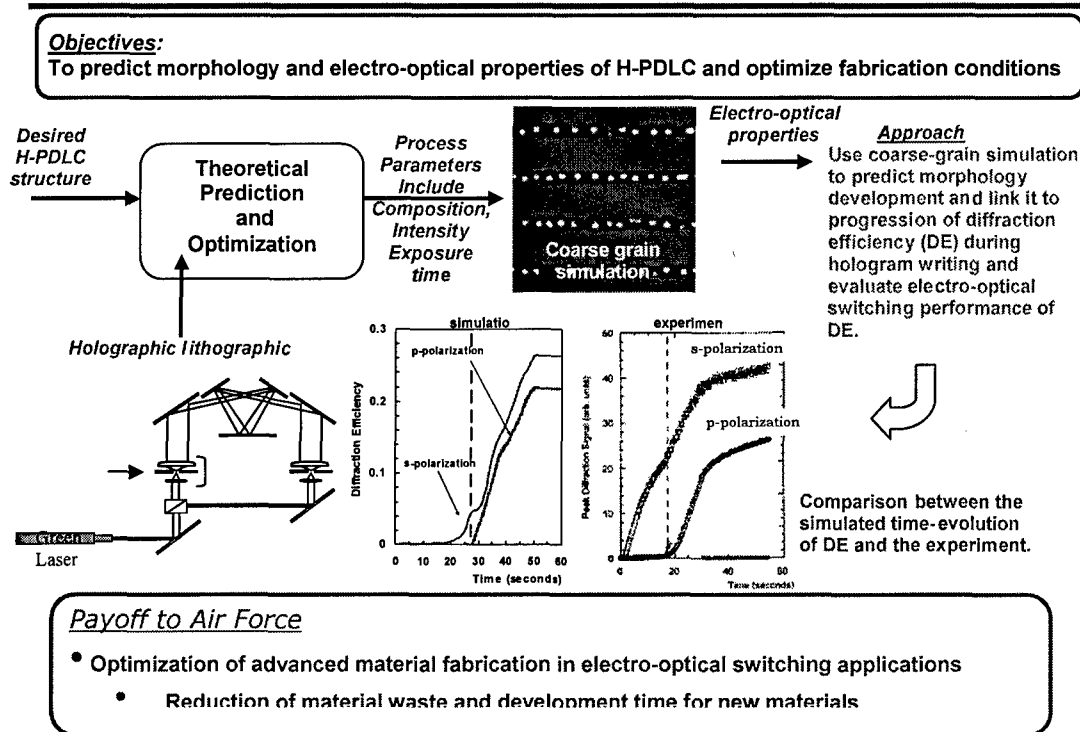**CNT based H-PDLC systems**

The PI's group is exploring, on a quantitative basis, the influence of external electric field on the switch-ability of fabricated tunable photonic crystals with and without carbon nanotube (CNT). The theoretical modeling and numerical simulation of this part is still in progress. We have performed the experimental part of the project in Bunning's laboratory at WPAFB. In the mean time, the PI's group has realized the orientation induced ordering in CNT/LC system. This study is the first to experimentally establish the chimney-type phase diagram of carbon nanotube and nematic liquid crystals caused by mutual alignment of the CNT and LC directors. A chimney-type phase diagram was identified in the multi-wall carbon nanotube (MWNT) /E7 mixture over a narrow range of 0.1–0.2% MWNT concentration. The isotropic–nematic phase transition temperature (TNI) of the liquid crystal component was found to enhance by the incorporation of MWNT within a small composition gap. This enhanced TNI phenomenon may be attributed to anisotropic alignment of liquid crystal molecules along the carbon nanotube bundles. This accomplishment has been reported: "Effect of carbon nanotube on phase transitions of nematic liquid crystals", H. Duran, B. Gazdecki, A. Yamashita, and T. Kyu, Liq. Cryst., 32, 815-822 (2005). At present, we are analyzing the preliminary results of CNT containing H-PDLC structures.

List of Publications
1. "Transport Controlled Pattern Photopolymerization in a Single-Component System." S. Meng, K. Nanjundiah, T. Kyu, L. V. Natarajan, V. P. Tondiglia, and T. J. Bunning, Macromolecules, 37, 3792-3798 (2004).
2. "Holographic photo-polymerization induced phase separation in reference to the phase diagram of a mixture of photo-curable monomer and nematic liquid crystal." S. Meng, T. Kyu, L.V. Natarajan, V. P. Tondiglia, R.L. Sutherland, and T.J. Bunning, Macromolecules, 38, 4844-4854 (2005).
3. "Effect of carbon nanotube on phase transitions of nematic liquid crystals", H. Duran, B. Gazdecki, A.Yamashita, and T. Kyu, Liq. Cryst., 32, 815-822 (2005).
4. "Holographic Polymer Dispersed Liquid Crystals and Polymeric Photonic Crystals formed by Holographic Photolithography," T. Kyu, S. Meng, H. Duran, K. Najundiah, and G.R. Yandek, Macromol. Res., 14, 155-165 (2006).

5. "Formation of Electrically Switchable Photonic Crystals via Various Optical Wave Interference Techniques" G.R. Yandek, S. Meng, G.M. Sigalov, and T. Kyu, Liq. Cryst., accepted (2006).

Theoretical modeling and simulation of H-PDLC fabrication via holographic lithography

Objectives:
To predict morphology and electro-optical properties of H-PDLC and optimize fabrication conditions

Desired H-PDLC structure → **Theoretical Prediction and Optimization** → *Process Parameters Include Composition, Intensity Exposure time*

Coarse grain simulation

Electro-optical properties

Approach
Use coarse-grain simulation to predict morphology development and link it to progression of diffraction efficiency (DE) during hologram writing and evaluate electro-optical switching performance of DE.

Holographic lithographic

Laser

Comparison between the simulated time-evolution of DE and the experiment.

Payoff to Air Force

- Optimization of advanced material fabrication in electro-optical switching applications
  - Reduction of material waste and development time for new materials

13

Summary on STW-21 project "Polymer Nanolithography"

PI: Dr. S. F. Lyuksyutov, AFRL POC: Dr. R. A. Vaia

Novel and alternative nano-patterning technique named atomic force microscopy electrostatic nanolithography (AFMEN) was developed. AFMEN generates features by mass transport of polymer within an initially uniform, planar film without chemical cross-linking, substantial polymer degradation or ablation. The combination of localized softening of attoliters (10^2-10^5 nm^3) of polymer by Joule heating, extremely non-uniform electric field gradients to polarize and manipulate the soften polymer, and single-step process methodology using conventional AFM equipment, establishes a new paradigm for polymer nanolithography, allowing rapid (order of microseconds) creation of raised (or depressed) features without external heating of a polymer film or AFM tip-film contact.
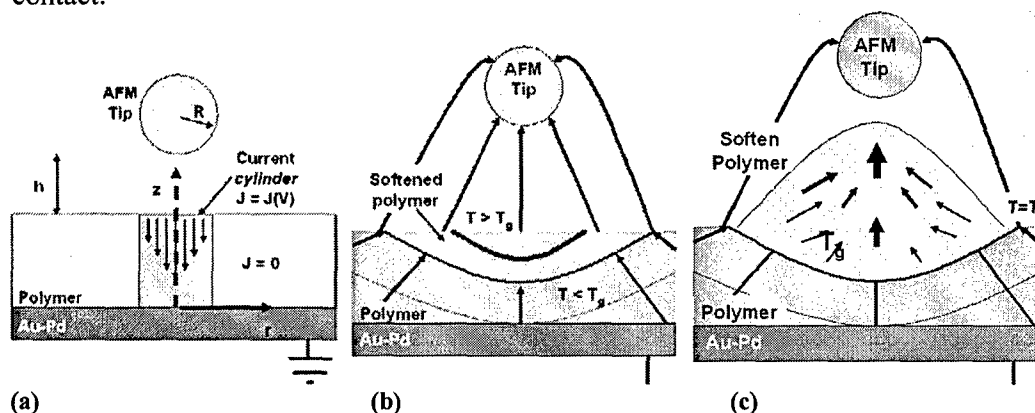

Figure 1: Conceptual presentation of the experimental layout and feature formation (not to scale): (a) Geometrical arrangement of AFM and polymer. Typical tip-surface distance is 0.5-5 nm and AFM tip radius is approximately 35 nm; (b) Isotherms (solid lines) within the polymer arising from Joule heating define volume of viscoelastic polymer. The highly non-uniform electric field (10^9 -10^{10} V/m) generates step electric field gradient (arrows). (c) The large non-uniform electric field gradient surrounding the AFM tip produces an electrostatic pressure on the polarizable, softened polymer creating raised features.

Friction at nanoscale between a conductive tip and non-conductive dielectric surface plays an important role for nanostructures formation. Our experimental study has confirmed the nanostructures in polymers can be formed *even without external bias* of AFM tips. Fine lines, 10-30 nm wide and 0.2-1 nm high, and nonoscopic dots can be patterned in 30-nm polymer film when the AFM tip either moves 0.3-1 nm or dwells above the surface for a short period of time ranging 0.1-1 s. The nanostructures' formation normally occurs as a result of AFM tip motion above the polymer surface with set point magnitude constraining the tip to come closer to the surface depending on the water meniscus size. A current of 100 pA −1 nA measured through the film was substantially smaller than that in AFMEN and is not accompanied by electric breakdown. Nano-lines and dots have been patterned with no applied electric voltage in PMMA and PS polymer films. Typical nanostructures using friction at nanoscale are presented in Figure 2.
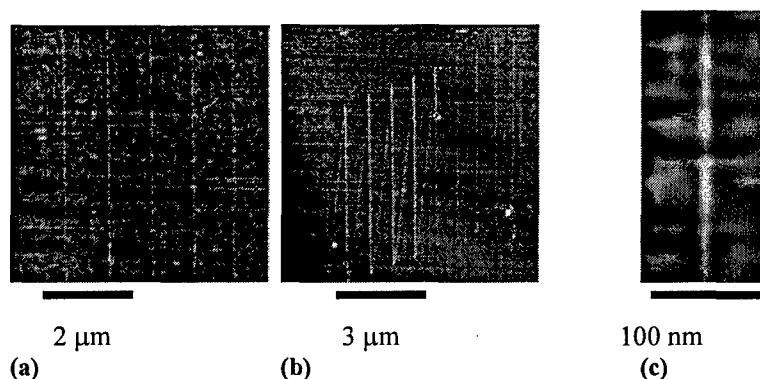
14

2 μm   3 μm   100 nm

(a)   (b)   (c)

Figure 2: Experimental results of nanostructures (lines) patterned in polymer films without external bias. (a) Lines of 25 nm wide and 0.8 nm high patterned in PMMA (ε=3.2, M_w = 528k, T_g = 115^0); AFM tip velocity was 1 μms^{-1} with the average current smaller than 100 pA; (b) Close-up of one of the lines; (c) Lines of 47 nm wide and 1 nm high patterned in PS (ε=2.6, M_w = 110k, T_g = 105^0) without external voltage: the nano-lines corresponds to lateral AFM tip motion above the surface;

Another practical outcome was development z-lift nanolithography (ZEN) in polymers. The technique was implemented experimentally by Mr. Juhl and Dr. Vaia at AFRL/MLBP. ZEN suggests the best repeatability for nanostructures formation in thin polymer films reported ever. It allows robust control of tip-surface separation (-5 – 150 nm) for specific variable parameters such as bias voltage and pulse duration. The technique concatenates the advantages of MILLIPIDE and AFMEN allowing fast (1-3 μs) nanodot formation, faster than any single-step existing lithography technique can pattern. Additional an advantage of z-lift lithography its relative independence on the chemical composition of the polymer film due to the absence of chemical cross-linking resulting in latent pattern formation: eleven polymers of different physical-chemical properties tested by this technique produced similar response.
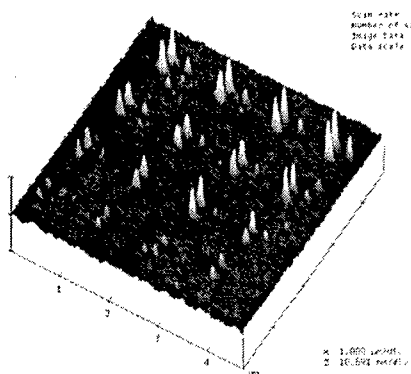

Figure 3: AFM image of an array viewed at 220° of dots patterned on a 40 nm thick 110k PS film containing three different processing parameters: voltage increase (-25 to -31V), voltage ramp increase for every column (0.01 s to 0.1 s), and four different z-lift values (-50, 0, +100, and +200) for every combination of voltage and pulse duration.

AFMEN technique was originally conceived at AFRL/MLBP in 2002 when PI worked as NRC Summer Faculty at AFRL/MLBP. During STW-21 funding period our joint Akron-USAF Team have filed 3 patens, published 6 refereed papers, 3 online preprints, and delivered more than 30 invited and contributed papers presented at APS, MRS, ACS and other meetings. The first refereed publication on AFMEN appeared in Lyuksyutov et al. [Nature Materials **2** 468-472 (2003)] and received press release in July 2003 by *Nature*

15

Publishing Group, and impact factor more than 40 by now. Additionally, AFMEN has been presented in *Nikkei Advanced Technology Report* (Japan) **50**, 11.24.2003, which is the mirror of Japan industry. In December 2003 PI was awarded Japan Society Promotion of Science Fellowship (equivalent of Humboldt fellowship in Germany): the success rate was 300 out of 1199).

Patents
S. Juhl, S. F. Lyuksyutov, and R. A. Vaia, "Z-lift nanolithography and uses thereof," U.S. **Patent provisional 60/606,597** (filing date 9.2.04)

S. F. Lyuksyutov, R. A. Vaia, S. Juhl, and P. B. Paramonov, "Method of amplitude modulated electrostatic nanolithography," **U.S. Patent 11/040,299** (under review 01.19.05)

S.F. Lyuksyutov, R.A. Vaia, and S. Juhl, "Method of Polymer Nanolithography," **U.S. Patent 10/817,406** (under review 3.25.04), Air Force invention number AFD 654, 05.22.03

Refereed publications during funding period (2003-2005)

S. F. Lyuksyutov, "Nano-patterning in polymeric materials and biological objects using atomic force microscopy electrostatic nanolithography," **Current Nanoscience** 1, 245-251 (2005)

P. B. Paramonov and S. F. Lyuksyutov, "Density functional description of water condensation in proximity of nanoscale asperity," **Journal of Chemical Physics** 123 084705 (2005)

S. Juhl, D. Philips, R. A. Vaia, S. F. Lyuksyutov, and P. B. Paramonov, "Precise formation of nanoscopic dots in polystyrene film using z-lift electrostatic nanolithography," **Applied Physics Letters** 85 3836-38 (2004)

S.F. Lyuksyutov, P.B. Paramonov, R.A. Sharipov, and G. Sigalov, "Induced deformations in polymers on nanoscale using atomic force microscopy," **Physical Review B** 70 (17), 174110, (2004)

S.F. Lyuksyutov, R.A. Vaia, P.B. Paramonov, and S. Juhl, "Amplitude-modulated electrostatic nanolithography in polymers based on atomic force microscopy," **Applied Physics Letters** 83 (21), 4405-4407 (2003)

S.F. Lyuksyutov, R.A. Vaia, P.B. Paramonov, S. Juhl, L. Waterhouse, R.M. Ralich, G. Sigalov, and E. Sancaktar, "Electrostatic nanolithography in polymers using atomic force microscopy," **Nature Materials** 2(7) 468-472 (2003)

Preprints and refereed proceedings

S. F. Lyuksyutov, S. B. Juhl, P. B. Paramonov, and R. A. Vaia, "Atomic force microscopy electrostatic nanolithography (AFMEN): Manipulation of thin polymer films under extreme electrostatic potentials," **Abstracts of papers of ACS 229**, U1124, 140-PMSE (2005)

S. F. Lyuksyutov, P. B. Paramonov, and R. A. Vaia "Free energy analysis of system comprising biased atomic force microscope tip, water meniscus, and dielectric surface," **arXiv: cond-mat/0505457**

P. B. Paramonov and S. F. Lyuksyutov, "Density functional description of water condensation in proximity of nanoscale asperity," **arXiv: physics/0504028**

S. F. Lyuksyutov, R. A. Sharipov, G. Sigalov, and P. B. Paramonov, "Exact analytical solution for electrostatic field produced by biased AFM tip dwelling above dielectric-conductor bi-layer", **arXiv: cond-mat/0408247**

S. F. Lyuksyutov, G. Sigalov, E. Sancaktar, P. B. Paramonov, and J. Kim, "A novel method of SPM-based nanolithography in polyethylene-terephthalate polymer films," **Polymer Surface Modification: Relevance to Adhesion 3**, 417-433 (2003) Ed. K.L. Mittal

Awards and distinctions received by Dr. S. F. Lyuksyutov as related to AFMEN

2005	**Buchtel College Early Career Research Award**, University of Akron, OH	
2004	**Japan Society for the Promotion of Science Fellow**, Institute of Technology, Japan	
2002-2004	**National Research Council Summer Faculty Fellow**, AF Research Lab, WPAFB, OH	

Collaborative Center in Polymer Photonics
Subproject: Simulations of Side-Chain Liquid Crystalline Polymers
Final Report July 21, 2006
Wayne L. Mattice
Alex Schulman Professor, Polymer Science, The University of Akron

I. GOALS/OBJECTIVES OF THE RESEARCH

The difficulty in equilibrating atomistically detailed models of polymers of photonic interest is well known. The problem is created by the fact that the longest relaxation time in the real system is far longer than the times accessible by conventional simulation methods such as Molecular Dynamics (MD). Our objective is the development of an alternative, faster approach using a different simulation methodology based on new bridging methods.

II. TECHNICAL APPROACH AND RESULTS

Two aspects of the new simulation methodology contribute to a more rapid equilibration of the model.

- The atomistically detailed model is replaced by a coarse-grained model. The reduction in the number of particles required to represent the system increases the speed of the simulation. Intramolecular constraints, derived from an atomistically detailed model for the chain, are imposed on the coarse-grained model. These constraints permit "reverse-mapping" of the equilibrated coarse-grained model to an atomistically detailed representation of the system.

- Equilibration of the coarse-grained model is achieved via a Monte Carlo (MC) simulation. In conventional MD simulations, the system must evolve to its equilibrium state via a physically accessible pathway. The MC simulation has access to alternative pathways that accelerate the equilibration. The use of nonphysical pathways in the MC simulation does not imply that the final equilibrated model is unphysical, because an equilibrium state (by definition) is independent of the route by which it is generated.

With NSF support, the parent bridging method was developed previously in our laboratory and applied to polymeric hydrocarbons in which coarse-grained beads were located at alternate carbon atoms in the backbone of the chain. A major challenge presented by the photonic polymers is the accurate incorporation into the coarse-grained model of large, densely arrayed side chains bearing chromophores (aromatic ring systems). The test case adopted was an asymmetrically substituted poly(silylenemethylene), $[Si(CH_3)R-CH_2]_x$, $R = -O(CH_2)_3OC_6H_4C_6H_5$. This molecule has the desired characteristics for a test case, namely, a large aromatic unit connected to the backbone by a flexible spacer. In addition, it is a molecule in which stereochemical composition is an issue. This feature is important, because it allows a test of whether the bridging method is sufficiently robust so that it allows the coarse-grained model to retain

18

the influence of stereochemical composition on the properties of the system. The bridging method represented each monomer unit with four beads. Since the monomer unit contains 40 atoms, the coarse-graining level (average number of atoms per bead) was 10.

The evolution of the coarse-graining level in our simulations is summarized in Table 1. In pre-CCPP work, we initially represented polyethylene with one bead for each C_2H_4 unit, and our initial simulation of a system where stereochemical composition is important used one bead for each C_3H_6 unit in polypropylene. In the initial CCPP work, the coarse-graining level was retained at a value close to our prior work with polypropylene, so that we could focus the new effort on the major challenge of the incorporation of the densely arrayed side chains with their chromophores and flexible spacers. The short-range intramolecular constraints on the coarse grained beads were derived from a rotational isomeric state description of the atomistically detailed model. Longer range constraints were derived from a discretized Lennard-Jones potential. Simulations with this coarse-grained model provided a reasonable dependence of the conformations on the stereochemical composition. They also suggested that the atactic chain may form a gauche helix in the solid state, which is in agreement with conclusion obtained earlier by experiment.

Table 1. Evolution of the successfully demonstrated level of coarse-graining

Publication Date	Coarse-graining (Atoms/bead)	Comment
1996-1997	6	Initial application, pre-CCPP [a]
2000	9	Initial application where stereochemical composition is important, pre-CCPP [b]
2004-2005	10	CCPP: first test case with aromatic group connected to backbone by a flexible spacer [c]
2006	32	CCPP: second test case [d]

[a] Rapold and Mattice, *Macromolecules* **1996**, *29*, 2457-2466. Cho and Mattice, *Macromolecules* **1997**, *30*, 637-644. Doruker and Mattice, *Macromolecules* **1997**, *30*, 5520-5526.
[b] Clancy, Pütz, Weinhold, Curro, and Mattice, *Macromolecules* **2000**, *33*, 9452-9463
[c] References 1-4 in Section IV.A of this report
[d] Reference 5 in Section IV.A of this report

Since the study of the poly(silylenemethylene) produced encouraging results, we then turned attention to ways of making the bridging method faster and more easily implemented.

- The increase in speed was sought by increasing the level of course graining (number of atoms represented by a bead) from 10 in the poly(silylenemethylene) to 32 in the new simulations. This change was achieved by exploiting the fact that the ultimate interest for CCPP is not in the conformations of the backbone, but is instead in the configurations adopted by the chromophores, which are located in the side chains. Therefore we retain only the coarse-grained beads located in the chromophores. The backbone remains present implicitly (but not explicitly),

because it still contributes to the intramolecular constraints on the coarse-grained beads.

- The greater ease of implementation was sought by mapping the new coarse-grained model onto the bond-fluctuation model, which is a very well known and widely employed simulation method first described in 1988 by Carmesin and Kremer. Since many laboratories have successful experience with the bond fluctuation model, a mapping onto this model facilitates use of our technique elsewhere.

The most recent tests with this new method demonstrate that it accurately retains the influence of stereochemical composition on the mean square dimensions in systems at bulk density, and also provides a strong acceleration of the equilibration of the model.

III. PERSONNEL

III. A. Personnel who received salary support from this account:
- Dr. Carin A. Helfer, Postdoc.
- Prof. Wayne L. Mattice, Alex Schulman Professor, Polymer Science

III.B. Personnel who contributed to the project, but with salary support from other accounts
- Prof. Donghai Chen, Visiting Professor. Professor, Department of Natural Science, Malone College, Canton, Ohio
- Dr. Numan Waheed, Postdoc.

III.C. Coauthor from Wright Patterson Air Force Base
- Dr. Barry L. Farmer

III.D. Citizenship
- All personnel named in Section III are US citizens

IV. PUBLICATIONS AND PRESENTATIONS

IV.A. Refereed Publications

(1) Carin A. Helfer, Wayne L. Mattice, and Donghai Chen, "Substituted Poly(silylenemethylene)s with Short Range Interactions That Induce a Preference for the Same Local Conformation in Unperturbed Atactic, Isotactic, and Syndiotactic Chains", *Polymer* **2004**, *45*, 1297-1306.
(2) Donghai Chen and Wayne L. Mattice, "A Monte Carlo Simulation of Coarse-Grained Poly(silylenemethylene) and Poly(dimethylsilylenemethylene) Melts", *Polymer* **2004**, *45*, 3877-3883.
(3) Carin A. Helfer, Donghai Chen, Wayne L. Mattice, and Barry L. Farmer, "Conformations Produced by Interaction of the Side Chains in the Poly(silylenemethylene) with Repeating Sequence $[Si(CH_3)R-CH_2]_x$, R = -

O(CH$_2$)$_3$OC$_6$H$_4$C$_6$H$_5$", *Journal of Polymer Science: Part B: Polymer Physics* **2005**, *43*, 886-896. Invited article in the special issue on Coarse Graining

(4) Wayne L. Mattice, Carin A. Helfer, Sagar S. Rane, Ernst D. von Meerwall, and Barry L. Farmer, "Come Mechanisms for Subtle Influences of Stereochemical Composition on the Physical Properties of Macromolecules", *Journal of Polymer Science: Part B: Polymer Physics* **2005**, *43*, 1271-1282. Invited Highlight Article.

(5) Wayne L. Mattice and Numan Waheed, "An Assessment of the Role of Quenched Randomness in the Stereochemical Sequences of Atactic Vinyl Polymers", *Macromolecules* **2006**, *39*, 2380-2387.

IV.B. Unrefereed Publications

(6) Carin A. Helfer and Wayne L. Mattice, "Extension of a Methodology for Lattice Simulations of a Single Chain to a Dense System for a Side Chain Liquid Crystal Polymer", *Polym. Mat. Sci. Eng. Prepr. (Am. Chem. Soc., Div. Polym. Mat. Sci. Eng.)* **2005**, *43*, 676.

(7) Wayne L. Mattice, Carin A. Helfer, and Barry L. Farmer, "Influence of Stereochemical Cmposition on an Asymmetrically Substituted Polysilylenemethylene", *Polym. Mat. Sci. Eng. Prepr. (Am. Chem. Soc., Div. Polym. Mat. Sci. Eng.)* **2005**, *43*, 834-835.

IV.C. Oral Presentations. Presenter's name underlined.

(8) <u>Carin A. Helfer</u> and Wayne L. Mattice, "Simulation of Side Chain Liquid Crystalline Poly(silylenemethylenes)", Wright Patterson Air Force Base, February 20, 2003. Poster

(9) <u>Carin A. Helfer</u> and Wayne L. Mattice, "Simulation of Coarse-Grained Chains", Wright Patterson Air Force Base, May 22, 2003. Lecture

(10) Carin A. Helfer, Donghai Chen, and <u>Wayne L. Mattice</u>, "Simulations of Side Chain Liquid Crystalline Polymers", Wright Patterson Air Force Based, August 21, 2003. Lecture

(11) <u>Carin A. Helfer</u>, Donghai Chen, and Wayne L. Mattice, "Application of a High Coordination Lattice to Investigate Side Chain Liquid Crystalline Polymers", Wright Patterson Air Force Base, August 21, 2003. Poster

(12) <u>Carin A. Helfer</u>, Donghai Chen, and Wayne L. Mattice, "Use of a High Coordination Lattice to Investigate Side Chain Liquid Crystalline Polymers", Molecular Modeling of Macromolecules Conference, Hilton Head Island, South Carolina, March 18-19, 2004. Poster

(13) <u>Carin A. Helfer</u>, Donghai Chen, and Wayne L. Mattice, "Molecular Modeling Studies to Investigate Ordered Structures of Side Chain Liquid Crystal Polymers for Photonic Applications", Polymer Photonics Workshop, Akron, April 22, 2004. Poster

(14) Carin A. Helfer, Donghai Chen, <u>Wayne L. Mattice</u>, and Barry L. Farmer, "Simulation of Side-Chain Liquid Crystalline Polymers", Collaborative Center for Polymer Photonics Annual Review, Akron, September 23, 2004. Lecture

(15) <u>Carin A. Helfer</u>, Donghai Chen, Barry L. Farmer, and Wayne L. Mattice, "Influence of Higher Order Intramolecular Interaction of the Chain Conformation of a Side Chain Liquid Crystal Polymer", Collaborative Center for Polymer Photonics Annual Review, Akron, September 23, 2004. Poster

(16) <u>Carin A. Helfer</u> and Wayne L. Mattice, "Extension of a Methodology for Lattice Simulations of a Single Chain to a Dense System for a Side Chain Liquid Crystal Polymer", National ACS Meeting, Washington, DC, August 30, 2005. Poster

(17) <u>Wayne L. Mattice</u>, Carin A. Helfer, and Barry L. Farmer, "Influence of Stereochemical Composition on an Asymmetrically Substituted Polysilylenemethylene", National ACS Meeting, Washington, DC, August 31, 2005. Lecture

07/19/2006

Synthesis of a novel *bis*(terpyridine) ligand, 4,4'-*bis*(2,2':6',2"-terpyridinyl)triphenylamine, utilizing triphenylamine, as a specific angle controller, has led to the self-assembly of a unique hexagonal metallomacrocycle family, [Fe$_6$(**1**)$_6$(PF$_6$)$_{12}$] and [Zn$_6$(**1**)$_6$(BF$_4$)$_{12}$],[1] utilizing terpyridine-metal(II)-terpyridine connectivity. The crystal structure of the novel ligand shows that the angle between the two terpyridyl moities is 119.69°, which enabled the formation of the hexagonal-shaped macrocycles. The crystal packing architectures of this starting ligand revealed channels induced by solvent encapsulation. Following complexation of this ligand with transition metals [Fe(II) or Zn(II)] in a one-pot reaction, the resultant structures were characterized by ^{1}H and ^{13}C NMR, UV/Vis, and mass spectroscopies.The expected metal-to-ligand charge transfer (MLCT; λ_{max} = 582 nm) and emission (λ_{em} = 575 nm) characteristics were exhibited by both [Fe$_6$(**1**)$_6$(PF$_6$)$_{12}$] and [Zn$_6$(**1**)$_6$(BF$_4$)$_{12}$] (Figure 1). The photoelectrochemical characteristics of these hexagonal metallomacrocycles demonstrate that they can be used as sensitizers in dye-sensitized solar cells.

Due to their light absorption properties, constructs **2** and **3** were also studied as sensitizer materials for solar cell devices. Photovoltaic experiments using dye-covered nanocrystalline TiO$_2$ electrodes (prepared by dipping the semiconductor substrate into a 0.2 mM MeCN solution of each hexamer) properly fitted in a solar cell device, were conducted using an AM 1.5 (100 mW·cm^{-2}) incident light source and an electrolyte containing 0.3M KI + 0.015M I$_2$ dissolved in a 4 to 1 ratio of propylene and ethylene carbonate. Discharge experiments conducted with these devices allowed the calculation of the following values. The fill factor (*ff*), the short circuit photocurrent (*J$_{sc}$*), as well as the open circuit photopotential (*V$_{oc}$*) for the Zn(II) metallomacrocycle, showed superior results over the Fe(II) metallomacrocycle. Further, the total photoconversion efficiency of the cell (*η*; 0.032 and 0.180 % for **2** and **3**, respectively) using electromagnetic radiation spanning the visible region of the spectrum exhibited better values than in the case of the Zn(II)

Figure 1
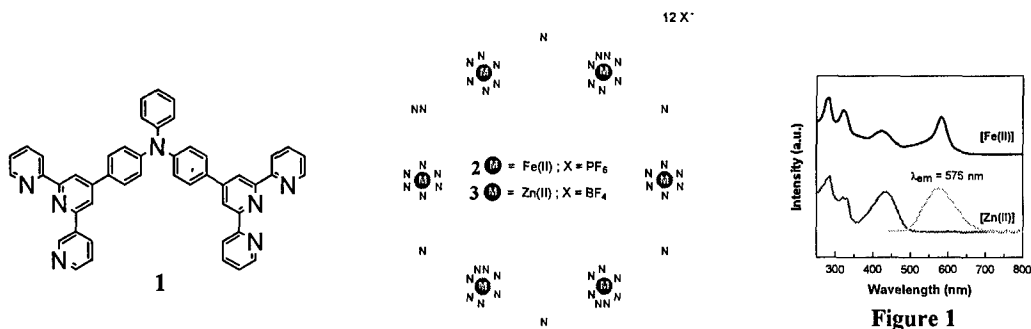
metallomacrocycle **3**.

We have demonstrated the formation and characterization of a series of unique, self-assembled, metallopentacycles.[2] Employing terpyridine-metal(II)-terpyridine connectivity, these complexes are stable and irreversible under the reaction conditions. The structures of these pentagonal architectures were characterized by means of ^{1}H and ^{13}C NMR, UV/Vis spectroscopy, and mass spectroscopy. Preliminary studies of photoelectrochemical performance for the metallopentacycles demonstrated their potential for solar cell development. Further experiments are currently ongoing to attain the electroluminescence behavior using LED device
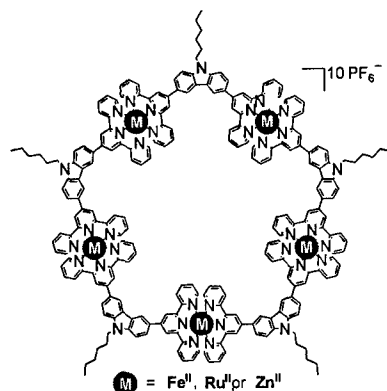

$\bar{\;}$10 PF$_6$

$\bigcirc$ = Fe^{II}, Ru^{II} or Zn^{II}

Table 1. Photovoltaic performances and surface coverage values of ITO/TiO$_2$/pentamer/KI-I$_2$ electrolyte/graphite dye-sensitized cells measured using a polychromatic 1.5 mW·cm^{-2} light source.

complex	j_{sc}^{a} (μA·cm^{-2})	V_{oc}^{b} (mV)	ff^{c} (%)	η^{d} (%)	$\Gamma/10^{-11, e}$ (mol·cm^{-2})
4 [Fe(II]	90.4	250	32.6	0.49	3.03
5 [Ru(II)]	300.4	290	26.3	1.53	5.49
6 [Zn(II)]	137.6	269	29.5	0.73	6.22

^{a}: short-circuit photocurrent density, ^{b}: open-circuit photovoltage, ^{c}: fill factor, ^{d}: photoconversion efficiency of the cell, ^{e}: surface coverage.

Due to their light absorption properties, these materials were also studied as sensitizer materials for solar cell devices. Photovoltaic performance experiments using dye-covered nanocrystalline TiO$_2$ electrodes (prepared by dipping the semiconductor substrate in a 0.2 mM MeCN solution of each one of the metallopentacycles) properly fitted in a solar cell device, were conducted using a polychromatic (1.5 mW·cm^{-2}) incident light source and an electrolyte containing 0.3M KI + 0.015M I$_2$ dissolved in a 4 to 1 ratio of propylene and ethylene carbonate. The surface coverage (Γ) of each metallopentacycle on the TiO$_2$ electrode was calculated using UV-vis spectroscopy experiments as reported by Grätzel.[35] Notably, the values obtained (Table 2) are fairly close to each other, thus supporting the similar structure and dimensions of compounds 4- 6. Discharge experiments conducted with these devices also allowed the calculation of some of the values in Table 1. Whereas the fill factor (ff) of the three electrodes studied here remains similar, the short circuit photocurrent (j_{sc}) as well as the open circuit photopotential (V_{oc}) for the Ru(II) metallopentacycle showed the best results. Also, total photoconversion efficiency of the cell (η) using electromagnetic radiation spanning the visible region of the spectrum exhibited the highest value in the case of the Ru(II) pentamer **5**.

An *O*-hexyl-3,5-*bis*(terpyridine)phenol ligand (**7**) has been synthesized and transformed into a hexagonal Zn(II)-metallomacrocycle[3] (**8**) by a facile self-assembly procedure capitalizing on terpyridine-Zn(II)-terpyridine connectivity. The structural composition was confirmed by NMR and mass spectral techniques; photo- and electroluminescence properties were also investigated. The OLED device shows green

electroluminescent emission at 515 nm with a maximum luminance of 39 cd/m^2 and maximum efficiency of 0.16 cd/A.
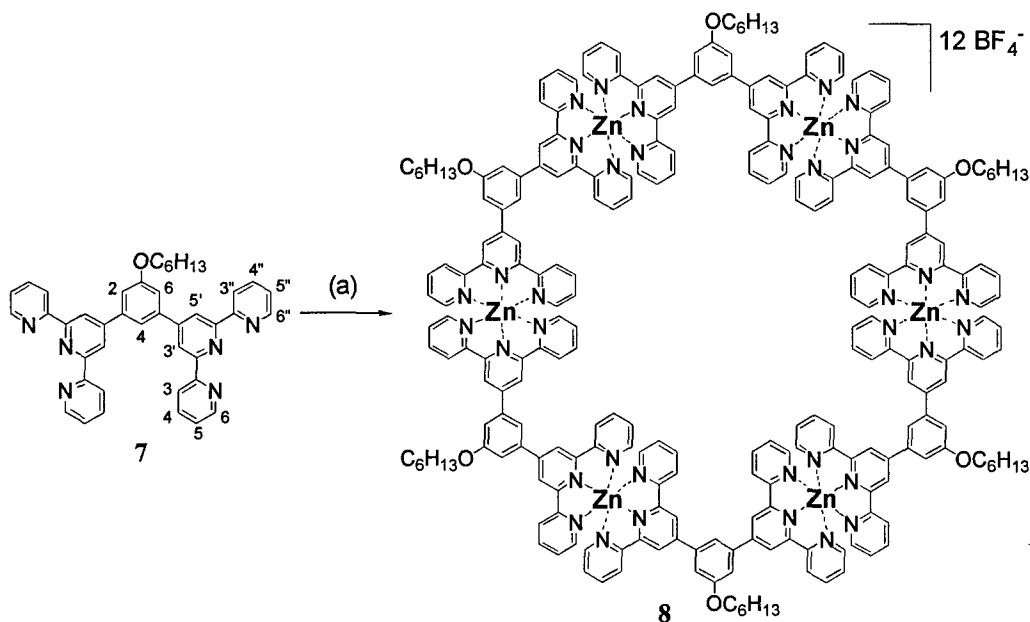
This Zn(II)-hexamer was fabricated into an electroluminescent device with the following configuration: ITO/PEDOT/NPD/Zn(II)-hexamer:BCzVBi/BCP/Alq$_3$/LiF/Al. Figure 2(A) schematically depicts the relative HOMO and LUMO energies of the components. The electroluminescence (EL) spectrum of this LED device at a bias voltage of 6.9 V shows an emission with peak maxima at 515 nm. [Figure 2(B)] At all forward-
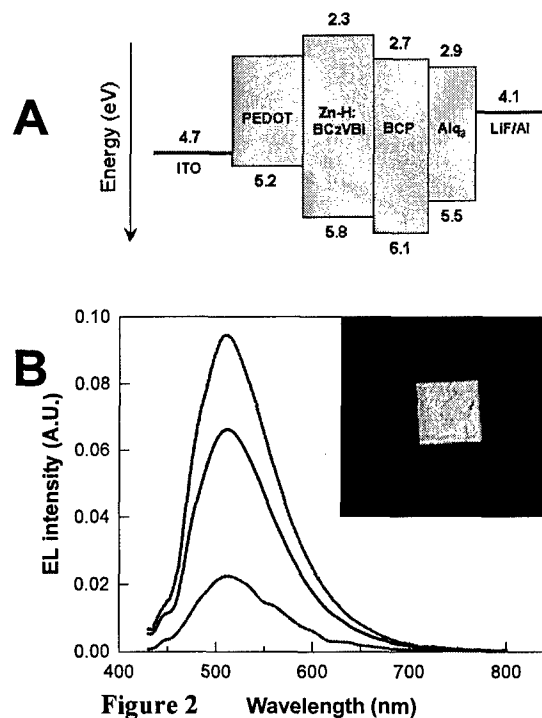

Figure 2   Wavelength (nm)

applied bias-voltages, only a green emission at λ_{max} = 515 nm was realized. These EL spectral results confirmed that the Zn(II)-hexamer functioned as an electron-transport material in the LED device. The current density-voltage-luminance (I-V-B) characteristics curve is shown in Figure 3. The turn-on voltage is ~4 V and the device has a maximum efficiency of 0.16 cd/A. The maximum luminance of 39 cd/m^2 was obtained under a driving voltage of 7.6 V. The emission color of the device is green (CIE coordinate: x = 0.28, y = 0.48).

Using the tenets of chemical self-assembly, the preparation of a non-dendritic, nano-scale, fractal molecule (i.e., **9**) based on Sierpinski's hexagonal gasket was prepared and characterized.[4] This non-dendritic, perfectly self-similar fractal macromolecule is comprised of *bis*terpyridine building blocks that are bound together by coordination to 36 Ru and 6 Fe ions to form a nearly planar array of increasingly larger hexagons around a hollow center.

In order to visually confirm the hexagonal structure, a droplet of an acetonitrile solution of **9** (100 µg/500 ml) was deposited on the surface of freshly cleaved mica or Au(111), dried under ambient conditions, and subjected to atomic force microscopy (AFM). This technique allows the mapping of a surface with a tip on a cantilever that results in a topographic image of a surface; the size and sharpness of the tip determines the size of the objects that can be mapped with good resolution. AFM provides data on a sample's dimensions including height. The AFM images of individual fractal constructs reveal an average diameter of 20 ± 2 nm, relative to the ca. 4 nm radius of curvature of the silicone tip used in the AFM measurements (Fig. 3A) thereby supporting the modeled diameter of ca. 12 ± 2 nm.. The higher magnification images exhibited clear patterns in which the six ruthenium hexamers and the central hole were clearly discernible.

Transmission electron microscopy (TEM; Fig. 3B) was also employed for characterization. TEM analysis provides the size, shape, and arrangement of a specimen and in some cases can provide crystallographic information. After casting a dilute methanol solution of **6** (250 µg/100 ml) on carbon-coated grids (Cu and Ni, 400 mesh), the resultant analysis showed the predicted fractal-like pattern (Fig. 3B) possessing an average diameter of 11 ± 1 nm for the single molecule, which gives direct evidence for the macrocyclization. Study of a higher magnification TEM image (Fig. 3B insert) reveals individual hexagonal gaskets lying flat or slightly tilted.

Ultra-high vacuum low-temperature scanning tunneling microscopy (UHV-LT-STM) was also employed to image the structure. This apparatus can generate images with atomic resolution by directly measuring electronic states. Ultra-high vacuum allows clean, controlled surface preparation and cryogenic temperatures to help reduce electronic noise and slow molecular motion. Using the same dilution employed for the TEM sample preparation, fractal construct **6** in acetonitrile was cast onto a freshly cleaned Au(111) surface. STM images acquired at 6 K (Fig. 3C) verified a hexagonal pattern of the molecule (12 ± 1 nm diameter, and ca. 0.8 nm in height), which was consistent with the computer-generated model of the structure. Tunneling conductance spectra determined for single molecules at 6 K showed a 1 eV energy gap. Traces of linear oligomeric as well as larger macrocyclic assemblies were also observed on the STM images.

Figure 3
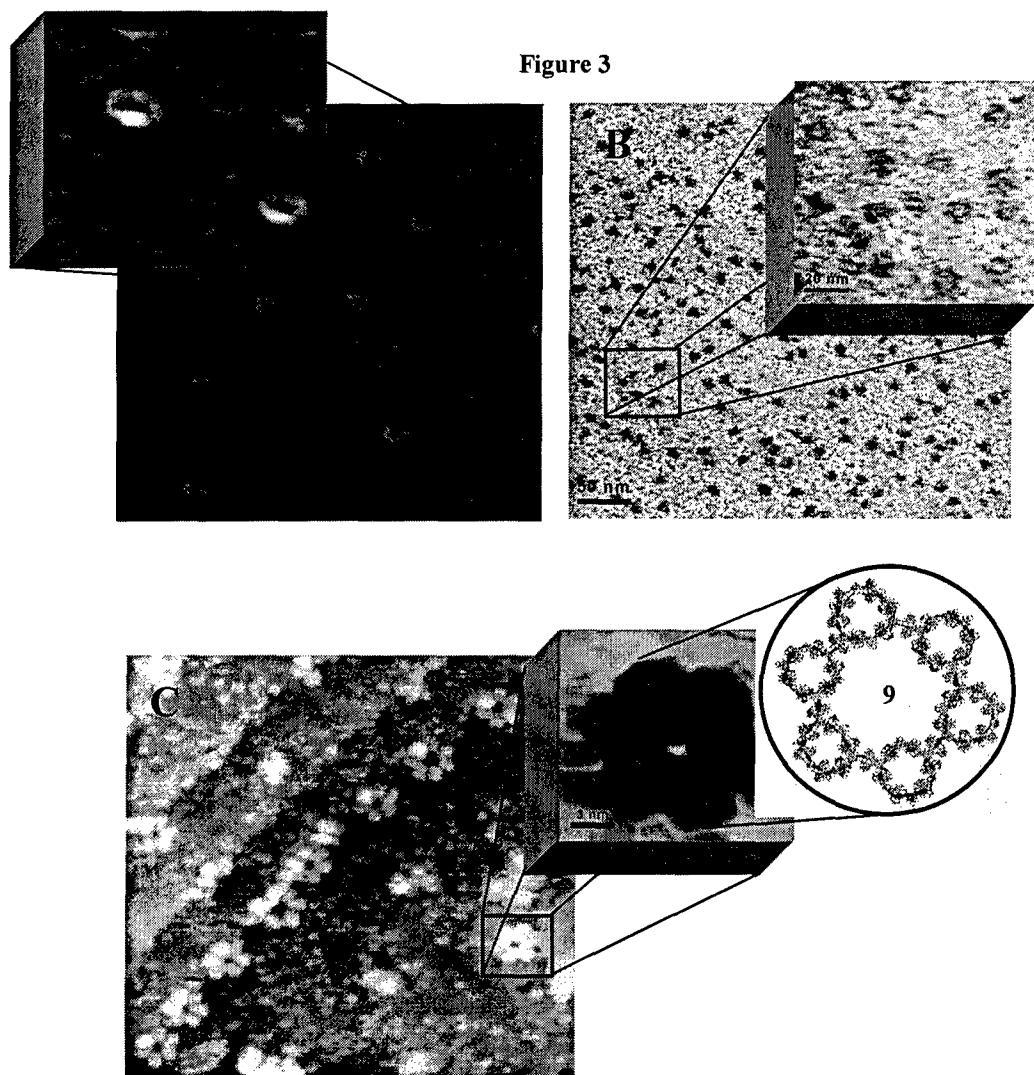
1. Hwang, S.-H.; Moorefield, C. N.; Wang, P.; Fronczek, F. R.; Courtney, B.; Newkome, G. R. "Design, synthesis and photoelectrochemical properties of hexagonal metallomacrocycles based on triphenylamine: [M6(4,4'-bis(2,2':6',2"-terpyridinyl)triphenyl)6(X)12]; [M = Fe(II) or Zn(II)]," *Dalton Trans.* **2006** 3518-3522.

2. Hwang, S.-H.; Wang, P.; Moorefield, C. N.; Godínez, L. A.; Manríquez, J.; Bustos, E.; Newkome, G. R. "Design, self-assembly, and photophysical properties of pentameric metallomacrocycles:" *Chem. Commun.* **2005**, (37), 4672-4674.

3. Hwang, S.-H.; Wang.P.; Moorefield, C. N.; Jung, J.-C.; Kim, J.-Y.; Lee, S.-W.; Newkome, G. R. "Construction of a Hexameric Zn(II)-Metallomacrocycle and Its

Photo- and Electroluminescence Properties: [Zn_6(*O*-hexyl-3,5-*bis*2,2':6',2"-terpyridine)phenol)$_6$(BF$_4$)$_{12}$]," *Unpublished results.* **2006**.

4. Newkome, G. R.; Wang, P.; Moorefield, C. N.; Cho, T. J.; Mohapatra, P. P.; Li, S.; Hwang, S.-H.; Lukoyanova, O.; Echegoyen, L.; Palagallo, J. A.; Iancu, V.; Hla, S.-W. "Nanoassembly of a Fractal Polymer: A Molecular "Serpinski Hexagonal Gasket"," *Science* **2006**, *312*, 1782-1785.

Synthesis of Block Copolymers for Photonics Applications

Roderic P. Quirk, Kumho Professor of Polymer Science
Michael Olechnowicz, Graduate Student
Maurice Morton Institute of Polymer Science
University of Akron
Akron, Ohio 44325

After consultation with Dr. Michael Durstock and his collaborators at The Materials & Manufacturing Directorate, Air Force Research Lab, Wright-Patterson Air Force Base on November 19, 2004, the consensus was that a viable synthetic goal for a useful diblock copolymer for photovoltaic applications would be well-defined poly(1,3-cyclohexadiene)-*block*-polylactide. Both of these blocks can be prepared by living polymerization to form well-defined block copolymers which will undergo spontaneous phase separation to form well-ordered, nanoscopic arrays. Cylindrical and bicontinuous interprenetrating morphologies were expected to be most useful and efficient for hole and electron transport.
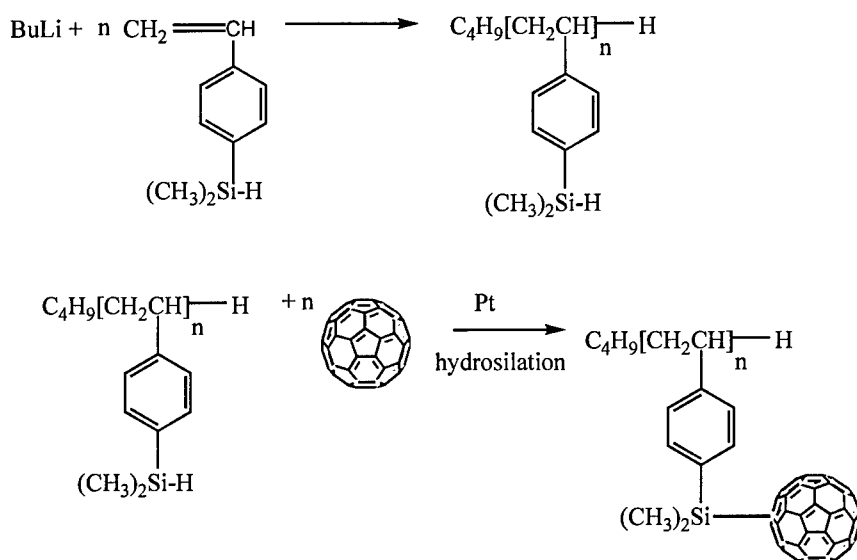
The anionic polymerization of 1,3-cyclohexadiene was utilized to formed 1,4-poly(1,3-cyclohexadienyl)lithium with controlled, variable molecular weights and narrow molecular weight distributions. These living polymers were functionalized with ethylene oxide to form ω-hydroxyethyl-1,4-poly(1,3-cylohexadiene), A, as shown in Scheme 1.
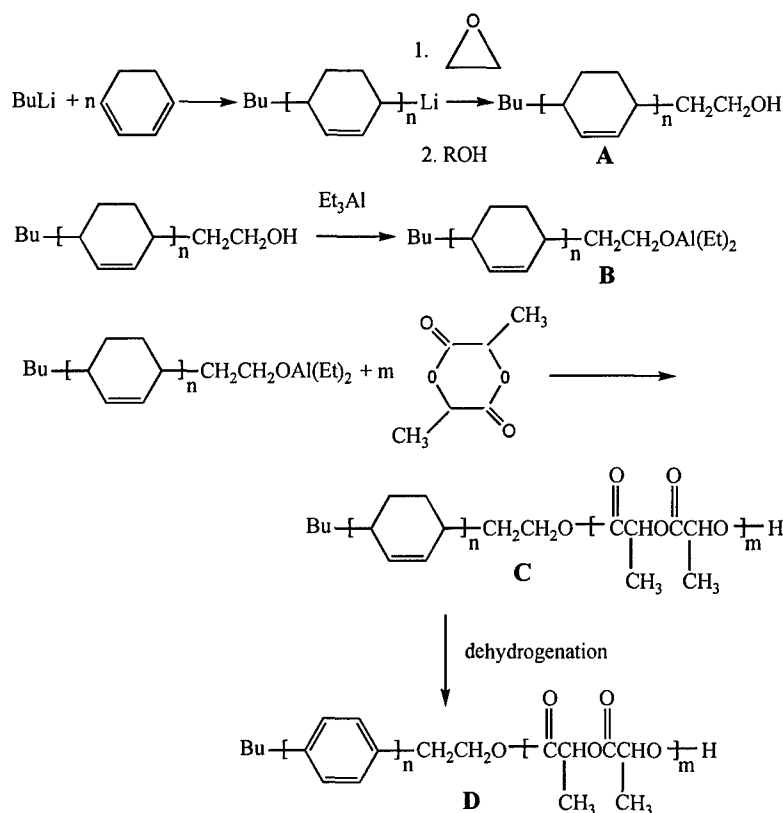
Scheme 1.

A series of hydroxyl-functionalized 1,4-poly(1,3-cyclohexadienes) were synthesized with well-defined structures (M_n = 4,100; 2,200; 16,00; $M_w/M_n \approx 1.1$). In order to obtain poly(p-phenylene) with high conjugation lengths (after dehydrogenation of poly(1,3-cyclohexadiene), it was necessary to prepare poly(1,3-cyclohexadiene) with high 1,4-stereospecificity. High field (700 MHz) ^{1}H NMR analysis showed that the microstructure was > 96 % 1,4. The hydroxyl-functionalized poly(1,3-cyclohexadienes) were reacted with triethylaluminum in a dry box to form the corresponding aluminum alkoxide initiator, **B**, for controlled, ring-opening polymerization of lactide to form the lactide diblock, **C**, as shown in Scheme 1. The molecular weights of the two blocks were chosen such that the polylactide block corresponded to 40 vol % which should result in phase separation into a morphology with cylinders of polylactide in a continuous matrix of polycyclo-hexadiene. [1] In this solid-state morphology, the 1,4-poly(1,3-cyclo-hexadiene) blocks were dehydrogenated with the quinones, tetrachloro-1,4-benzoquinone and 2,3-dichloro-5,6-dicyano-1,4-benzoquinone, to form the corresponding poly(4-phenylene) block copolymer, **D** [2]. After dehydrogenation, the polylactide block in D was to be removed in the solid state using methanolic NaOH to form poly(p-phenylene) matrix with porous, cylindrical domains. Finally, a dispersion of C_{60} was be imbided into the porous poly(p-phenylene) matrix. Before the project was terminated after one year, the desired diblock copolymers were prepared, and the polyphenylene block was formed with high conjugation length (λ_{max} = 343 nm corresponding to 41 phenylene units).

Block copolymers with covalently attached fullerenes (C_{60}). As an alternative to the physical incorporation of fullerene into the pores of a semiconducting matrix as described above, it was envisioned that a well-defined, phase-separated block copolymer with covalently attached fullerene units could also be prepared by living anionic polymerization coupled with hydrosilation chemistry. Well-defined block copolymers composed of a semi-conducting block and a second block with covalently attached fullerene groups should be very effective materials for photovoltaic applications. We began an investigation to develop a general method for attaching a variety of substituents to polymer chains using hydrosilation chemistry.[5,6] We wanted to explore the use of this chemistry to attach fullerene molecules to polymer chains as side-chain substituents as shown in Scheme 2. Buckminsterfullerene (C_{60}) has been attached to the monomer, 2,4,6,8-tetramethylcyclotetrasiloxane [7] and to the polymer, polymethylhydridomethyl-octylsiloxanea) [8], via hydrosilation with platinum catalysts. These studies provided precedent for expecting that this chemistry would be analogous for the corresponding polystyrene backbones. As a first step in developing materials for photovoltaic applications, we carried out the butyllithium-initiated polymerization of (4-vinylphenyl)dimethylsilane as shown in the first step in Scheme 2. The resulting polymerization is a controlled polymerization: the M_n (calc) $\approx M_n$ (obs) and $M_w/M_n \leq 1.1$. Using hydrosilation chemistry for attaching fullerenes to polymer blocks would have provided a methodology for investigating what structural features optimize photovoltaic responses for block copolymers containing a semi-conducting block connected to a covalently attached, fullerene-containing block. The controlled, presumably living, nature of the butyllithium-initiated polymerization of (4-vinylphenyl)dimethylsilane would provide the methodology for preparation of block copolymers of this monomer with semiconducting blocks from monomers such as 2-phenyl-1,3-cyclohexadiene (after

30

BuLi + n CH$_2$=CH $\longrightarrow$ C$_4$H$_9$[CH$_2$CH]$_n$—H

(CH$_3$)$_2$Si-H   (CH$_3$)$_2$Si-H

C$_4$H$_9$[CH$_2$CH]$_n$—H + n $\xrightarrow[\text{hydrosilation}]{\text{Pt}}$ C$_4$H$_9$[CH$_2$CH]$_n$—H

(CH$_3$)$_2$Si-H   (CH$_3$)$_2$Si—

Scheme 2.

aromatization). The fullerene-containing block can also be attached to a semi-conducting, substituted polythiophene using the controlled polymerization procedures developed by the groups of McCullough [9] and Rieke [10].

References

[1] Bates, F. S.; Fredrickson, G. H. *Ann. Rev. Phys. Chem.* **1990**, *41*, 525.
[2] Williamson, D. T.; Buchanan, T. D.; Elkins, C. L.; Long, T. E. *Macromolecules* **2004**, *37*, 4505.
[3] Johnson, B. J. S.; Wolf, J. H.; Zalusky, A. S.; Hillmyer, M. A. *Chem. Mater.* **2004**, *16*, 2909.
[4] Kovacic, P.; Hsu, L. C. *J. Polym. Sci., Polym. Chem. Ed.* **1966**, *4*, 5.
[5] Quirk, R. P.; Roy Chowdhury, S. *Polym. Prep. (Am. Chem. Soc., Div. Polym. Chem.)* **2005**, *46*(2), 585.
[6] Quirk, R. P.; Kim, H.; Polce, M.; Wesdemiotis, C. *Macromolecules* **2005**, *38*, 7896.
[7] Miller, M. L.; West, R. *Chem. Commun.* **1999**, 1797.
[8] Segura, J. L.; Martin, N.; Guldi, D. M. *Chem. Soc. Rev.* **2005**, *34*, 31.
[9] Chen, F.; Mehta, P. G.; Takiff, L.; McCullough, R. D. *J. Mater. Chem.* **1996** *6*, 1763.
[10] Sandstedt, C. A.; Rieke, R. D.; Eckhardt, C. J. *Chem. Mater.* **1995**, *7*, 1057.

Development of Optical Techniques for Materials Characterization at the Nanoscale

Summary of Results and Achievements for 3 years (9.2002-8.2005)
(Groups of Drs. A.P. Sokolov and M.D. Foster, The University of Akron, in collaboration with: *J. Maguire, R. Vaia,* Air Force Research Laboratory)

Materials characterization at the nanoscale is extremely important for development of new photonic and electronic technologies. There are, however, not many traditional techniques that can provide characterizations at so small scales. In particular, key to the development of many photonic structures and devices is the nanoscale characterization of chemical composition. However, the spatial resolution of commercially available techniques typically used for chemical characterization is not sufficient to address nanoscale structures. Raman spectroscopy is a particularly attractive technique for characterizing chemistry because it is also sensitive to polymer chain conformation as well as stresses in materials. In this work Raman spectroscopy and scanning probe imaging have been combined to create an apertureless imaging technique that provides Raman spectroscopic study of surfaces with unprecedented lateral resolution.

The method is based on Raman spectroscopy combined with apertureless near field nano-optics. The latter is based on strong and local enhancement of optical signals in the vicinity of modified (usually coated by Au and/or Ag) scanning probe tips. We have constructed the spectrometer with side-illumination optics and performed experiments that demonstrate clearly the feasibility and strength of the approach [1-3]. We are developing technology of the AFM tip modification that provides significant enhancement of the Raman signal in the vicinity of the apex due to optical plasmon resonance. We have demonstrated significant signal enhancement for a broad variety of materials: small organic molecules (Methylene Blue, R6G), semiconductors (CdS, Si), polymers, and carbon nanotubes (Fig.1) [1,2]. We achieved reproducible ~10^4 times enhancement of the Raman signal by Au and Ag coated tips. We found that Au-coated tips keep stable enhancement for a period of 2-3 months. We estimated localization of the Raman signal enhancement to be ~20 nm [1]. All these *results prove the principle of the proposed scanning nano-Raman spectrometer.*

One of the main challenges in broad use of the nano-Raman spectroscopy is relatively low contrast of near-field to far-field (background) signal, because the achieved enhancement factor (~10^4 times) is not sufficient in many cases. We have developed a method based on optimization of polarization geometry and incident angle of the side-illumination optics that provides increase of contrast ~50 times in the case of Si [1,3]. A patent has been filed for this development. *These achievements make the technique attractive for various applications.*

We are currently developing a non-contact scanning mode that uses a tuning fork instead of a conventional AFM cantilever. Another important development is design of the plasmon-based tips with higher enhancement factors. Resonant excitation of surface plasmons of a metal or metal-coated tip is most effective when the optical spectrum of the tip is matched to the excitation wavelength. However, prior to our work the optical spectrum of a tip with sub-wavelength dimensions had not been successfully measured. We have developed [4,5] a technique based on total internal reflection microscopy to measure the optical properties of tips (Figure 2).
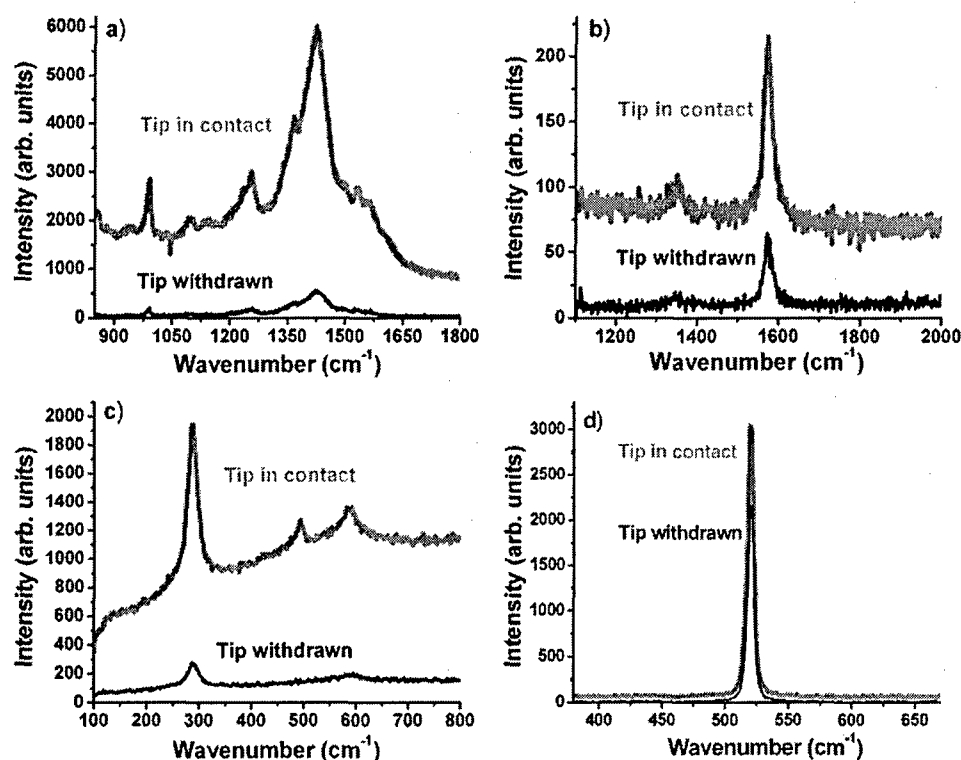
Figure 1: Comparison of the spectra measured with tip withdrawn (far-field signal only) and gold-coated tip in contact (far-field plus near-field) for: (a) Poly(3,4-ethylenedioxythiophene) poly(styrenesulfonate) (PEDOT/PSS) polymer film measured with λ=647 nm, apparent enhancement ~9; (b) monolayer of SWNT measured with λ=514 nm, apparent enhancement ~3; (c) 10 nm CdS film, apparent enhancement ~6, and (d) Si wafer measured with λ=514 nm, apparent enhancement ~1.4.

We demonstrated [4,5] that moving the wavelength of light into the resonance of the tip provides higher tip enhancement. This technology opens possibility for controlled design of the aperture-less tips with high enhancement factors, the key element of the nano-Raman instrument. This is an important step in the *design of nano-photonic devices*.

Another part of our research has been related to use of *GHz-THz light scattering spectroscopy* (Brillouin and Raman scattering) *for analysis of nano-structured and nano-composite materials*. Using this spectroscopy, we have developed a method

for measuring mechanical properties and their anisotropy in nano-structured materials. No change in mechanical
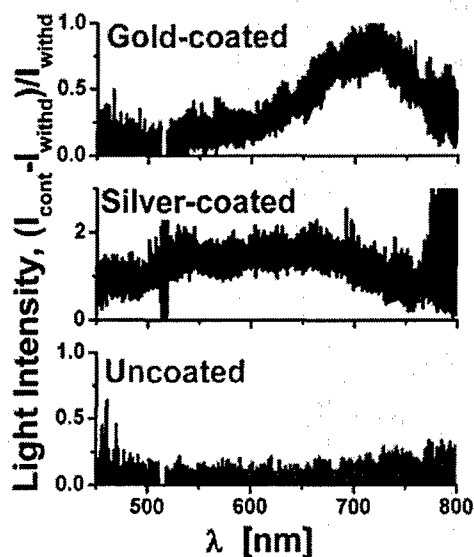

Figure 2: Optical scattering spectra for a) gold-coated, b) silver-coated and c) uncoated Si_3N_4 tips. The gap in the range ~510 – 520 nm is due to the notch filter for the 514.5 nm laser.

33

properties and no anisotropy have been detected down to the length scale of ~80 nm in structures created by advanced lithographic techniques [6,7]. Our results advanced understanding of phononics in small objects that can be applied to analysis of other nano-structures, including photonic crystals, colloidal systems, nano-assemblies of viruses, etc. We are also studying microscopic mechanism of mechanical reinforcement in polymer – carbon nanotubes (CNT) composite materials [8]. By adding only ~1% CNT, we achieved 3 fold enhancement of Young's modulus in polypropylene. Detailed microscopic analysis, using Raman spectroscopy under mechanical load, confirms good load transfer from polymer matrix to CNT and leads us to conclude that a 1% concentration of CNT was enough to reach the percolation threshold.

The results of the work have been presented on *APS* March 2004, *MRS* 2004 and *ACS Fall* 2004 meetings, *Polymer Photonics Workshop* (April 2004), *Polymer West* Gordon Research conference 2005 and some other meetings. The results are published in 8 papers [1-8], and one patent has been filed [9].

References:
1. D. Mehtani, N. Lee, R. D. Hartschuh, A. Kisliuk, M.D. Foster, A. P. Sokolov, J. F. Maguire, *Nano-Raman Spectroscopy with Side-illumination Optics*, **J. Raman Spectr. 36**, 1068 (2005).
2. N. Lee, J.S. Lee, A. Kisliuk, A. Sokolov, M.D. Foster, *Surface segregation of blends of highly branched PS studied using surface enhanced Raman scattering*, **Polymeric Materials Science and Engineering 91**, 649 (2004).
3. D. Mehtani, N. Lee, R. D. Hartschuh, A. Kisliuk, M.D. Foster, A. P. Sokolov, J. F. Maguire, *"Tip-enhanced Raman spectroscopy with high contrast"*, **Proc. SPIE v. 5927**, 592707 (2005).
4. D. Mehtani, N. Lee, R. D. Hartschuh, A. Kisliuk, M.D. Foster, A. P. Sokolov, I. Tsukerman, *"Optical properties of the tips for apertureless near-field microscopy"*, **Proc. SPIE v. 5927**, 59270K1 (2005).
5. D Mehtani, N Lee, R D Hartschuh, A Kisliuk, M D Foster, A P Sokolov, F Čajko and I Tsukerman, *"Optical properties and enhancement factors of the tips for apertureless near-field optics"*, **J. Optics A: Pure and Appl. Optics 8**, S183 (2006).
6. R. Hartschuh, Y. Ding, J. H. Roh, A. Kisliuk, A. P. Sokolov, C. L. Soles, W. -l. Wu, A. P. Mahorowala, *Brillouin Scattering Studies of Polymeric Nanostructures*, **J.Polym.Sci. B 42**, 1106 (2004).
7. R. D. Hartschuh, A. Kisliuk, V. Novikov, A. P. Sokolov, P. R. Heyliger, C. M. Flannery, W. L. Johnson, C. L. Soles, W. L. Wu, *"Acoustic Modes and Elastic Properties of Polymeric Nanostructures"*, **Appl. Phys. Letters 87**, 173121 (2005).
8. T.E. Chang, L.R. Jensen, A. Kisliuk, R.B. Pipes, R. Pyrz, A.P. Sokolov, *"Microscopic mechanism of reinforcement in single-wall carbon nanotube / polypropylene nanocomposite"*, **Polymer 46**, 439 (2005).
9. A.P. Sokolov, A. Kisliuk, D. Mehtani, R. Hartschuh, N.H. Lee, Patent Application *"High Contrast Tip-Enhanced Raman Spectroscopy"*.